

THE MARIANA SCHUSTER (Orcid ID : 0000-0002-3836-0242)

DR DIANE GAIL OWEN SAUNDERS (Orcid ID : 0000-0003-2847-5721)

DR VIVIANNE VLEESHOUWERS (Orcid ID : 0000-0002-8160-4556)

DR YUANCHAO WANG (Orcid ID : 0000-0001-5803-5343)

DR SUOMENG DONG (Orcid ID : 0000-0002-9623-6776)

Article type : - Regular Manuscript

Cleavage of a pathogen apoplastic protein by plant subtilases activates host immunity

Shuaishuai Wang¹, Rongkang Xing¹, Yan Wang^{1,6}, Haidong Shu¹, Shenggui Fu¹, Jie Huang¹, Judith K. Paulus², Mariana Schuster², Diane G.O. Saunders^{3,4}, Joe Win³, Vivianne Vleeshouwers⁵, Yuanchao Wang^{1,6}, Xiaobo Zheng¹, Renier A. L. van der Hoorn², Suomeng Dong^{1,3,6,*}

¹Department of Plant Pathology, Nanjing Agricultural University, Nanjing, 210095, China.

²The Plant Chemetics Laboratory, Department of Plant Sciences, University of Oxford, South Parks Road, Oxford OX1 3RB, United Kingdom.

³The Sainsbury Laboratory, University of East Anglia, Norwich Research Park, Norwich NR4 7UH, United Kingdom.

⁴John Innes Centre, Norwich Research Park, Norwich, NR4 7UH, United Kingdom.

⁵Wageningen UR Plant Breeding, Wageningen University and Research Centre, Droevendaalsesteeg 1, Wageningen 6708 PB, The Netherlands.

This article has been accepted for publication and undergone full peer review but has not been through the copyediting, typesetting, pagination and proofreading process, which may lead to differences between this version and the [Version of Record](#). Please cite this article as [doi: 10.1111/NPH.17120](https://doi.org/10.1111/NPH.17120)

This article is protected by copyright. All rights reserved

⁶The Key Laboratory of Plant Immunity, Nanjing Agricultural University, Nanjing, 210095, China.

*Corresponding author: Tel: 86-25-84395513; Email: smdong@njau.edu.cn.

ORCID ID: 0000-0002-7927-3583 (S.W.); 0000-0001-7465-5518 (Yan Wang); 0000-0002-9769-8278 (H.S.); 0000-0001-6791-6548 (J.P.); 0000-0002-9851-2404 (J.W.); 0000-0002-8160-4556 (V.V.); 0000-0001-5803-5343 (Yuanchao Wang); 0000-0002-3692-7487 (R.H.); 0000-0002-9623-6776 (S.D.).

Received: *5 October 2020*

Accepted: *19 November 2020*

Brief heading

Cleavage of a pathogen apoplastic protein activates immunity

Abstract

The plant apoplast is a harsh environment in which hydrolytic enzymes, especially proteases, accumulate during pathogen infection. However, the defense functions of most apoplastic proteases remain largely elusive.

We show that a newly identified small cysteine rich secreted protein PC2 from the potato late blight pathogen *Phytophthora infestans* induces immunity in *Solanum* plants only after cleavage by plant apoplastic subtilisin-like proteases, such as tomato P69B.

A minimal 61-amino-acid core peptide carrying two key cysteines, conserved widely in most oomycete species, is sufficient for PC2-induced cell death. Furthermore, we showed that Kazal-like protease inhibitors, such as EPI1 produced by *P. infestans* prevent PC2 cleavage and dampen PC2 elicited host immunity.

This study reveals that cleavage of pathogen proteins to release immunogenic peptides is an important function of plant apoplastic proteases.

Key words: *Phytophthora*; small cysteine rich effector; PC2; apoplast; cleavage; serine protease; P69B; immunity.

Introduction

The plant apoplast is the extracellular compartment serving as a major battlefield for plant-pathogen interactions (Du *et al.*, 2016). To defend against invading microbes, plants have evolved pattern recognition receptors (PRRs) to recognize microbe-associated molecular patterns (MAMPs) in the apoplastic interface and activate innate immunity (Boller & He, 2009; Miao *et al.*, 2019). MAMPs comprise a wide category of molecules such as bacterial flagellin, elongation factors, peptidoglycan, and fungal cell wall chitin (Newman *et al.*, 2013). Recently, apoplastic proteins have been recognized as an exciting resource for identifying new MAMPs. Some of these proteins are effectors that act to break down plant extracellular immunity through their biochemical functions. However, the peptide signatures of these proteins can also be recognized by plant membrane-localized PRRs to trigger a series of immune responses including reactive oxygen species (ROS) production, defense-related marker gene expression or hypersensitive cell death (Jones & Dangl, 2006). These proteins such as necrosis and ethylene-inducing protein (NEP) and xyloglucan-specific endoglucanase (XEG) are evolutionarily conserved across microbial taxa, providing an opportunity to study broad spectrum plant-microbe apoplastic interactions (Gijzen & Nurnberger, 2006; Ma *et al.*, 2015). However, the mode of action of most apoplastic proteins remains largely elusive. Revealing the mechanisms at play in the plant apoplastic space during microbial infection can provide novel insight into pathogenesis and identify new targets for engineering more robust plant immunity.

The plant apoplast is a harsh environment which is full of digestive enzymes including proteases. Several plant proteases are highly up-regulated during pathogen infection and have long been tied to plant immunity. One such example is the tomato subtilisin-like serine protease P69B, which was first reported as a pathogenesis-related (PR) protein (Tornerio *et al.*, 1997). Other evidence pinpoints apoplastic proteases as important players in plant immunity. For instance, silencing the papain-like cysteine protease (PLCP) C14 orthologs in *Nicotiana benthamiana* leads to increased plant susceptibility to *Phytophthora infestans*, the causal agent of potato late blight (Kaschani *et al.*, 2010). Moreover, depletion of PIP1, a PLCP in tomato, results in hyper-susceptibility to fungal, bacterial, and oomycete diseases, demonstrating that PIP1 constitutes a basal defense to a wide range of pathogens (Ilyas *et al.*, 2015).

Apoplasmic proteases act in plant immunity in either protease activity-dependent or independent manners. Rcr3, a PLCP that is closely related to PIP1, is essential for the receptor Cf-2 to recognize the apoplasmic effector Avr2 from *Cladosporium fulvum*, which acts as a PLCP inhibitor (Krüger *et al.*, 2002). However, inhibition of Rcr3 activity using the PLCP inhibitor E-64 does not trigger Cf-2-mediated HR, suggesting Cf-2 triggered plant immunity is independent of Rcr3 activity (Rooney *et al.*, 2005). In contrast, a recent study demonstrates that the release of the maize immune signaling peptide Zip1 requires maize PLCPs. In this case, PLCP activity activates SA immune signaling and maize resistance to the maize pathogen *Ustilago maydis* (Ziemann *et al.*, 2018). Plant genomes encode a large family of proteases with distinct predicted activities. Identifying the substrates of these proteases is critical to uncover their mode of action. However, the substrates of most proteases remain unclear. Although the underlying mechanisms are far from clear, current findings demonstrate that plant proteases play an important role in the regulation of plant immunity.

Inhibition of plant proteases represents a general counter-defense strategy used by invading pathogens (Wang *et al.*, 2020). To achieve successful colonization, adapted microbial pathogens deliver protease inhibitors into the host apoplast to counteract host defense. For example, fungal apoplasmic effector Pit2 secreted by *U. maydis* inhibits a set of apoplasmic maize cysteine proteases implicated in maize defense and contributes to the virulence of *U. maydis* in maize (Mueller *et al.*, 2013; Misas Villamil *et al.*, 2019). In *Phytophthora*, a well-characterized group of intercellular protein is the extracellular cystatin-like protease inhibitors (EPIC). *P. infestans* EPIC1 binds to tomato PLCP Rcr3 and C14 and inhibits their activity in the tomato apoplast (Kaschani *et al.*, 2010). EPIC2B is a more robust cysteine protease inhibitor with stronger inhibitory activity against Rcr3 and PIP1 (Dong, S. *et al.*, 2014). Beside *Phytophthora* EPIC2B and fungal Avr2, Gr-Vap1 from cyst nematode and Cip1 from pathogenic *Pseudomonas bacteria* also target these tomato proteases (Misas Villamil *et al.*, 2019), indicating that different pathogens have independently evolved divergent effectors to inhibit plant proteases during co-evolution. In addition, *P. infestans* secretes Kazal-like serine protease inhibitors, including the EPI1 and EPI10 proteins that inhibit tomato subtilase P69B (Tian *et al.*, 2004; Tian *et al.*, 2005). More recently, a study on the pathogenicity of Huanglongbing uncovered the *Candidatus Liberibacter asiaticus* effector SDE1 that directly interacts with and inhibits citrus PLCP activity (Clark *et al.*, 2018). In another case, the cyst nematode *Heterodera schachtii* effector

protein 4E02 repurposes a PLCP from its role in defense by targeting it to distinct plant cell compartments without inhibiting its activity (Pogorelko *et al.*, 2019). These studies illustrate a concerted interaction between the host proteases and the pathogen protease inhibitors, which dictates the success of pathogen colonization.

Interestingly, one common signature of apoplastic proteins is the presence of cysteine residues, which likely form disulfide bonds within the effectors to maintain their stability and biochemical function under harsh plant extracellular conditions. An early study on fungal avirulence effectors led to the characterization of small cysteine rich (SCR) proteins which are typified by their rich content of cysteine residues and small molecular weight (Templeton *et al.*, 1994). In other plant pathogens such as oomycetes, SCR proteins form a major group of apoplastic effectors (Torto *et al.*, 2003). PcF, an SCR effector secreted by *Phytophthora cactorum* induces necrosis in plants (Orsomando *et al.*, 2001). Another SCR effector SCR74 was identified in *P. infestans*, and the genes encoding SCR74 family of effectors are under strong diversifying selection (Liu *et al.*, 2005).

In this study, we developed a pipeline to identify potential SCR proteins in *P. infestans* and performed a high-throughput SCR proteins functional screen in *N. benthamiana* for immune response. We identified the SCR protein PC2, that is capable of triggering plant immune responses in a manner typical of MAMP. Further investigation revealed that PC2 is proteolytically cleaved by plant serine proteases such as tomato P69B. Genetic manipulation of P69B and chemical inhibition of serine protease activity both act to impair PC2-triggered immunity, suggesting that the cleavage process is essential for PC2-triggered plant immunity. In addition, we found that the cleavage could be suppressed by EPs, the *Phytophthora* Kazal-like protease inhibitors. This study highlights an example that a plant protease cleaves a pathogen apoplastic protein to activate defense responses to achieve immunity, and the pathogen may deploy protease inhibitors as a counter-defense measure to evade recognition by the host.

Materials and Methods

Identification of candidate apoplastic effectors

The predicted secretome of *P. infestans* was previously defined (Raffaele, Sylvain *et al.*, 2010) and each of the 1,412 secreted proteins annotated herein based on features typical of known effector

proteins (Table S1). This included: (i) identification of Pfam domains using batch searches with default parameters (Sonnhammer *et al.*, 1997), (ii) sequence similarity searches across the *Phytophthora* species cluster representing clade 1c species (Raffaele, S. *et al.*, 2010), searches across *Phytophthora* species in general and searches against a list of core *P. infestans* orthologs (Haas *et al.*, 2009) using BlastP searches with e-value cutoffs of 10^{-5} , (iii) classification of small cysteine-rich proteins that were defined as those less than 200 amino acids in mature protein and having a cysteine number greater than or equal to 4 and a cysteine content higher than 5% (Stergiopoulos & de Wit, 2009), (iv) sequence similarity searches across the predicted secretomes of an array of fungal plant pathogens with e-value cutoffs of 10^{-5} , (v) presence/absence of the RxLR motif using a custom perl script, (vi) analysis of gene expression during mycelium, sporangia, and infection stages (Raffaele, Sylvain *et al.*, 2010; Ah-Fong *et al.*, 2017; Chen *et al.*, 2018), (vii) sequence similarity analysis with species in the oomycete genus *Salisapilia* using BlastP searches with e-value cutoffs of 10^{-5} , and (viii) presence of genes in gene sparse regions in the *P. infestans* genome as described previously (Saunders *et al.*, 2012) (Table S1). These classified as being expressed in hyphae and planta and encoding small cysteine rich (SCR) proteins were selected for functional analysis as putative apoplastic effector candidates (Table S2).

Growth of plants and microbes

All plants were grown in pots containing the mixture of sterile soil and vermiculite (1:1) at 25°C under a 16-hours-light/8-hours-dark condition. *Escherichia coli* strain DH5 α was used to propagate plasmids and express secreted proteins. *Agrobacterium tumefaciens* strains GV3101 was used for agroinfiltration in plants. *P. infestans* strain T30-4 was routinely maintained in rye medium at 18°C under dark condition.

Molecular cloning and bioinformatic analysis

Full-length *PC2* (selected from the Table S2 (PITG_14439)) and its orthologs (Table S3) were cloned with *PR1* signal peptide into the reconstructive PVX vector pICH31160 for immunity test *in planta*. *PC2* mutants were also cloned with *PR1* signal peptide into the vector pICH31160 for immunity test *in planta*. *P69s* and *EPIs* genes were cloned into the plant expression vector pICH86988. Tobacco Rattle Virus (TRV)-based vector pTRV1 and pTRV2e were used for gene silencing in *N.*

benthamiana. Plasmid pFLAG-ATS (Sigma) was used for protein expression in *E. coli*. All the constructs and primers pairs were listed in Table S4 and S5.

To determine the presence of PC2 orthologs, we performed a blastp search in the Eumicrobe DB (<http://www.eumicrobedb.org/eumicrobedb/index.php>) (Panda *et al.*, 2018). Signal peptide prediction was performed using the SignalP 4.1 server (<http://www.cbs.dtu.dk/services/SignalP/>). Molecular phylogenetic analysis was performed using neighbour-joining (NJ) algorithm with support analysis (1,000 replicates) included in MEGA (v7.0) (<https://www.megasoftware.net/>) with default parameters based on the Poisson correction model. The *N. benthamiana* and tomato subtilases were described in recent studies (Paulus *et al.*, 2020). The potato subtilases were previously described in (Norero *et al.*, 2016). All complete subtilases were aligned using Muscle and distance matrices are clustered using UPGMA.

Transient expression *in planta*

A. tumefaciens-mediated transient expression in *N. benthamiana* was performed using 4-week-old plants. To test whether PC2 and its orthologs trigger cell death in *N. benthamiana*, GV3101 strains carrying PC2 or its orthologs (OD=0.5) and the P19 silencing suppressor (OD=0.1), were infiltrated into *N. benthamiana* leaves. To test the induction of cell death in other *Solanum* plants, Nep1-like protein (NLP), empty vector (EV) and PC2 (OD=1.0) were infiltrated into leaves. VIGS experiments were conducted using *A. tumefaciens* strains harboring the pTRV1 (OD=0.5) and the corresponding pTRV2 vector (OD=0.5) on two-week-old *N. benthamiana* plants. The silencing efficiency was measured by quantitative real-time polymerase chain reaction (qRT-PCR) and the silenced plants were used for the cell death test.

RNA isolation and qRT-PCR analysis

The RNA isolation and qRT-PCR analysis were carried out as previous reported (Huang *et al.*, 2019). The amplification specificity for each sample solution was verified by melting curve analysis in Fig. S1

Cell death analysis

N. benthamiana leaves were exposed under UV light (365 nm) in ultraviolet imager (Tanon 5200 Multi) at five days post agroinfiltration. The raw image was used for cell death intensity statistics

using ImageJ software and for coloring by TanonImage software. Each treatment had at least three replications.

Oxygen burst detection

Oxygen burst was evaluated based on H₂O₂ accumulation after staining *N. benthamiana* leaves with diaminobenzidine (DAB) using the previously reported protocol (Song *et al.*, 2015). Leaves were collected for DAB staining at two days post agroinfiltration. Specific experimental method was carried out as reported.

Extraction of the recombinant protein from plant tissues

For the proteins with coding sequences cloned into the plant expression vectors (pICH31160 and pICH86988) were expressed in *N. benthamiana*. The power of leaves was added to an extraction buffer (10% glycerol, 25 mM Tris pH 7.5, 1 mM EDTA, 150 mM NaCl), 10 mM dithiothreitol, protease inhibitor cocktail (1:100, Sigma) and 0.15% NP-40. Samples were centrifuged at max speed for 10 min at 4°C, and the supernatant was used for SDS-PAGE. *N. benthamiana* apoplastic fluids were harvested using phosphate buffered saline (PBS) buffer (NaPO₄ 50 mM, NaCl 150 mM, pH 7.0) (Dong, Suomeng *et al.*, 2014). For tomato leaves, a 0.24 M sorbitol solution was used as an extraction buffer (de Wit & Spikman, 1982).

Expression and enrichment of recombinant proteins from *E. coli*

For the proteins with coding sequences cloned into the pFLAG-ATS vector were expressed in *E. coli* (Kamoun *et al.*, 1997). Culture filtrate was harvested based on the protocol described in Dong et al (Dong, S. *et al.*, 2014). The recombinant proteins with either FLAG-tag or His-tag were purified by corresponding immune affinity agarose beads (Sigma).

***In vitro* PC2 proteolytic cleavage assay**

P69B protein was extracted from *N. benthamiana* apoplastic fluids using PBS (PH=5.5), and 10 µl extract was incubated with recombinant PC2 (1 µM) purified from *E. coli* in 50 µl volume at 10°C for 30 min. The reaction products were detected by SDS-PAGE using anti-FLAG and anti-HA.

***In vitro* and *in vivo* protease inhibition assay**

For inhibition assay *in vivo*, each chemical inhibitor was infiltrated into *N. benthamiana* leaves 6 hours before PC2 agroinfiltration. Inhibitors used in this work included DPI (Sigma, 10 μ M), Protease inhibitor cocktail (Sigma, 1%), and 3,4-Dichloroisocoumarin (DCI, Sigma, 1 mM) were dissolved in DMSO. LaCl₃ (Sigma, 10 mM), AEBSF (Sigma, 1 mM), E-64 (Sigma, 10 μ M) were dissolved in H₂O. For inhibition assay of EPI effectors from *P. infestans*, we infiltrated *Agrobacterium* strains carrying PC2 36 hours after EPIs agroinfiltration.

Inhibition of serine protease activity in tomato and *N. benthamiana*, apoplastic fluids were assessed using an active-site probe for serine proteases (Liu *et al.*, 1999). First, 50 μ L apoplastic fluid was pre-incubated with DCI (1 mM), E-64 (10 μ M) or the same volume of DMSO for 30 min. Then, labelling of active serine proteases was performed by incubating 43 μ L apoplastic fluid with 5mM sodium acetate (NaOAc), 5 mM DTT and 0.2 μ M FP-Tamra (Thermo) for 1 h at room temperature in the dark. After incubation, the labelled proteins were acetone-precipitated and separated by 14% SDS-PAGE. Labelled proteins were visualized by in-gel fluorescence scanning using a Typhoon FLA 9000 scanner.

For *in vitro* proteolytic cleavage assay of PC2 by P69B, the serine protease inhibitor DCI was used to block P69B activity. The DCI (0.5 mM, 1 mM, or 2 mM) was pre-incubation with PC2 (1 μ M) protein 30 min before P69B protein was added into the tubes. To detect the inhibitor activity of EPI1a *in vitro*, we incubated purified EPI1a or EPI1b (1 μ M, 5 μ M, or 25 μ M) with P69B for 30 min followed by incubation with PC2 (1 μ M) for 30 min at 10°C. The reaction products were detected by immunoblotting with anti-FLAG and anti-HA.

Results

Identification of the *P. infestans* SCR protein PC2

To identify candidate *P. infestans* apoplastic proteins as MAMPs for further investigation, we established a bioinformatic pipeline to predict putative apoplastic proteins from the *P. infestans* secreted proteome (Saunders *et al.*, 2012). A total of 65 SCR proteins were predicted based on characteristics typical of apoplastic effectors such as the presence of a secretion signal, a high number of cysteine residues, and small protein size (Fig. 1a, Table S1). Among these genes, 37 encode known elicitor, cellulose-binding elicitor lectin (CBEL), and protease inhibitor homologs. Next, we evaluated

the expression of the other 28 candidate SCR proteins using publicly available gene expression data (Ah-Fong *et al.*, 2017). This analysis identified a subset of five genes encoding predicted SCR proteins that were highly expressed during mycelium, sporangia, and infection stages (Table S2). Therefore, we focused on these five candidate SCR proteins for further evaluation.

To investigate the biological function of these five candidate SCR proteins, we carried out the ectopic expression assay in *N. benthamiana*. Five genes were cloned and assembled with the 35S promoter and *Nicotiana* pathogenesis-related protein 1 (PR1) signal peptide for secretion (Fig. S2a). Effector expression in *N. benthamiana* was performed utilizing the potato virus X (PVX) transient expression system mediated by *A. tumefaciens*. At five days post-agroinfiltration, ectopic expression of three candidate SCR genes triggered cell death in *N. benthamiana* (Fig. 1b,c). Among these genes, PITG_14439 (designated PC2), encoding an SCR protein containing 18 cysteine residues (Fig. S2b) and is conserved among all the *Phytophthora* species we examined so far (Table S3), shows a strong and stable cell death phenotype (Fig. 1b,c) and normal protein accumulation (Fig. S2c). To further evaluate the expression of PC2 during infection we carried out qRT-PCR. *P. infestans* strain T30-4 was used to inoculate Heinz tomato leaves and samples were collected at nine time points ranging from 3 hpi to 120 hpi. Transcript levels were measured by qRT-PCR using the *P. infestans* beta-tubulin gene as the internal reference. The qRT-PCR analysis illustrated that PC2 is up-regulated during infection, peaking at 48 hours post infection (Fig. S3a). *Avr3a* is significantly induced during the biotrophic stage whereas *NPPI.1* is a marker gene for the necrotrophic stage during *P. infestans* infection (Armstrong *et al.*, 2005; Kavroulakis *et al.*, 2006). In our assay, both *Avr3a* and *NPPI.1* expression patterns are consistent with previous publications, suggesting our sampling and qRT-PCR process is comparable (Fig. S3b).

PC2 induced plant immune response

To study the biological activity of PC2 protein, we transiently expressed PC2 with HA or His tags and evaluated its role in inducing cell death in *N. benthamiana*. The well-studied elicitor gene *INF1* served as a positive control. According to the result, tags don't interfere with the function of PC2 (Fig. 2a,b). Transient expression of PC2 in *Solanum lycopersicum*, *S. melongena*, and *S. tuberosum* induced typical cell death or necrosis symptoms (Fig. S4). However, transient expression of PC2 in *N. tabacum* does not give a strong phenotype. Given that NLP control does not give a robust cell death in

our assay, we cannot reach a clear conclusion whether PC2 functions in *N. tabacum*. Nevertheless, these results suggest that PC2 is able to trigger cell death in a wide range of *Solanum* species. To further evaluate PC2-triggered plant responses, we examined ROS accumulation after PC2 expression in *N. benthamiana*. Staining with DAB showed that PC2 expression leads to a high level of ROS accumulation (Fig. 2c,d). In addition, qRT-PCR assays demonstrated that the defense-related genes *PR1* and *RbohB* were significantly up-regulated in response to PC2 expression (Fig. 2e). Furthermore, the application of the ROS inhibitor DPI or calcium channel inhibitor LaCl₃ blocked PC2-induced cell death (Fig. 2f,g).

Pattern-triggered immunity relies on the recognition of plant pattern recognition receptors (PRRs). Next we evaluated whether PC2-induced immunity requires a PRR co-receptor by evaluating PC2-induced cell death in *BAK1* and *SOBIR1* silenced *N. benthamiana* plants (Heese *et al.*, 2007; Liebrand *et al.*, 2013). PC2-induced cell death was only impaired in *BAK1*- but not *SOBIR1*- silenced plants (Fig. 2h,i and S5a,b), indicating that *N. benthamiana* perception of PC2 likely requires the co-receptor BAK1. Furthermore, we scored PC2-induced cell death on *N. benthamiana* plants with individually silenced different defence-related genes including *SGT1*, *EDS1*, *NDRI*, and *RARI*. Our data demonstrate that PC2-induced cell death requires *SGT1*, but not *EDS1*, *NDRI*, or *RARI* (Fig. S6). Together these results indicate that PC2-induced immune responses require calcium burst and ROS production and highly dependent on plant membrane-associated LRR-RK as PRR.

PC2 orthologs are widely present in oomycete species

To determine the presence of PC2 orthologs in oomycetes, we performed a blastp search in the Eumicrobe database (Panda *et al.*, 2018). PC2 orthologs were identified in *Phytophthora*, downy mildew, *Salisapilias*, and *Pythium* genomes (Table S3). The proteins encoded by these homologs varied in length, but all carried signal peptides and conserved cysteine residues (Fig. 3a and S7). However, we failed to detect any homologous sequence from *Albugo* genomes. Phylogenetic analysis revealed that PC2 and its orthologs from *Phytophthora* spp. and *Peronophythora* spp. form a clade distinct from those of other oomycetes, with the orthologs from *Hyaloperonospora arabidopsidis* and *Pythium* being the least related relatives (Fig. 3a).

To determine the function of the PC2 orthologs, the orthologs from *P. sojae*, *Peronophythora litchii*, *H. arabidopsidis* and *P. ultimum* were cloned and transiently expressed in *N. benthamiana*.

The orthologs from *P. sojae* (PsPC2) and *P. litchii* (PlPC2) triggered visible cell death, while the orthologs from *H. arabidopsidis* (HpaPC2) and *P. ultimum* (PyuPC2) didn't induce cell death phenotype (Fig. 3b,c). Immunoblot analysis using an HA antibody confirmed that PC2 and its orthologs were successfully expressed in *N. benthamiana* leaves (Fig. 3d). These data indicate that the PC2 orthologs in oomycetes are conserved but show functional divergence.

A core minimal peptide of PC2 and two conserved cysteine residues are required for PC2 activity

The conservation of sequence and the diversity in function of PC2 orthologs prompted us to identify the sequence signatures that are required for PC2-induced cell death. Based on the predicted secondary structure of the PC2 protein, PC2 mutants designated from PC2^{M1} to PC2^{M5} were constructed and transiently expressed in *N. benthamiana* (Fig. 4a). In this way, narrowed down the functional PC2 fragment to a region between amino acids 138-198 (Fig. 4b,c). The cognate PC2 mutant was designated as PC2^{M3}, which elicited even stronger cell death when compared with the full-length PC2. In contrast, the PC2^{M4} or PC2^{M5} mutants, which were further reduced in size, lost full activity in triggering cell death (Fig. 4a,b). In line with our finding that HpaPC2 does not trigger cell death in *N. benthamiana*, the HpaPC2^{M1} mutant with the corresponding peptide matching to PC2^{M3}, doesn't have such function. To confirm the minimum PC2 functional peptide sequence, we conducted a gain-of-function assay through testing the ability of the HpaPC2 mutants to induce cell death (HpaPC2^{M2} to HpaPC2^{M3}). These two chimeric PC2 mutants gained cell death-inducing activity (Fig. 4a,b), suggesting that the epitope containing the 138-198 amino acids of PC2 is pivotal to induce plant defense responses.

The minimal functional fragment of PC2 contains seven cysteine residues (Fig. S8a). To determine whether these cysteines play a role in maintaining effector structure and are essential for PC2-induced cell death, we replaced these cysteines alone or together with alanine in PC2^{M3} and produced 8 mutants (PC2^{M3}(C146A), PC2^{M3}(C152A), PC2^{M3}(C161A), PC2^{M3}(C177A), PC2^{M3}(C183A), PC2^{M3}(C189A), PC2^{M3}(C198A), and a mutant carries all the above seven sites mutation PC2^{M3}(7CA)). Cell death assays were carried out in *N. benthamiana* and substitution of the cysteine residue at position 183 or 189 was shown to impair cell death, suggesting these two residues are required for this function (Fig. S8b,c). To further confirm these results, we substituted cysteine residues at positions 183 and/or 189 with

alanine in the full-length PC2 and generated three mutants (PC2^{M6}, PC2^{M7}, and PC2^{M8}). All mutants lost their cell death activity when tested in *N. benthamiana* (Fig. 4a,b), although western blots confirmed the corresponding proteins remained stable (Fig. 4c). Remarkably, the two cysteine residues at positions 183 and 189 are conserved in all PC2 orthologs. Thus, our PC2 mutagenesis assay demonstrates that the region from 138 to 198 and the two conserved cysteine residues in this region are required for PC2 function in triggering cell death in *N. benthamiana*.

Plant serine protease P69B mediates cleavage of PC2 protein

We found that PC2^{M3} mutant trigger stronger cell death than PC2 full length in the previous experiment (Fig. 4a), so we examined whether PC2 protein was processed to generate bioactive peptides. We infiltrated a plant protease inhibitor cocktail into *N. benthamiana* following transient expression of PC2. This significantly impaired PC2-triggered cell death (Fig. 5a). To figure out which component of cocktail suppressed PC2-triggered cell death, we infiltrated each individual component into *N. benthamiana* leaves six hours before transient expression of PC2. Cell death was strongly inhibited by serine protease inhibitor DCI, whereas the other protease inhibitors such as cysteine protease inhibitor E-64 did not inhibit PC2-induced cell death (Fig. 5a,b and S9). Thereby, we reasoned that PC2 may be cleaved by serine proteases to produce bioactive peptides, which can be later recognized by the plants. To identify candidate plant proteases suppressed by DCI, we monitored the activity of serine proteases in the apoplast of tomato and *N. benthamiana* using the fluorophosphonate activity-based probe FP-TAMRA. Preincubation of the apoplast extract with DCI strongly suppressed labeling of 70 kDa subtilases in apoplastic fluid in both plant species (Fig. 5c). This suggests that subtilases might be required for PC2-induced cell death, with P69B as a likely candidate is the most abundant subtilase displayed with FP-TAMRA in the apoplastic fluid of tomato (Sueldo *et al.*, 2014).

To explore whether the activity of P69B is required for PC2 cleavage, we performed an *in vitro* cleavage experiment. The apoplastic fluid from *N. benthamiana* leaves transformed with the EV control resulted in weak cleavage of PC2, but no such event was observed in PBS buffer (Fig. 5d). This data indicates that PC2 can naturally be cleaved in *N. benthamiana* extracellular proteases. Apoplastic fluid fractions from P69B expressing leaves showed a very clear cleavage of PC2 that was not found when expressing P69A, P69D, or P69F, suggesting that PC2 is specifically cleaved by

P69B. Furthermore, we co-incubated PC2 protein with different concentrations of P69B with different incubation times. The data showed that when we add the same amount of PC2 protein, the degradation of PC2 was increased with increasing abundance of P69B or incubation time (Fig. 5e,f). To confirm that P69B cleaves PC2 in a protease activity-dependent manner, we introduced the DCI inhibitor in a co-incubation *in vitro* experiment. We found that PC2 cleavage was attenuated with increasing DCI concentrations (Fig. 5g,h). However, DMSO, solvent of DCI, only weakly affected PC2 cleavage at high concentrations. Together, these data illustrate that the serine protease P69B cleaves PC2 *in vitro* in a protease activity-dependent manner.

Serine protease P69B is required for PC2-triggered immunity

To address the question of whether PC2 cleaved by P69B is required for PC2-induced cell death activity, we grew the tomato asP69B line, a previously reported *P69B* silenced tomato line (Paulus *et al.*, 2020). Here, we used qRT-PCR to examine *P69B* expression and confirmed the silencing of *P69B* in the asP69B line (Fig. 6a). We then extracted the apoplastic fluids from asP69B and wild-type (WT) lines. Recombinant PC2 protein was cleaved when co-incubated with apoplastic fluid from WT plants but not when co-incubated with apoplastic fluid from asP69B plants (Fig. 6b).

To test if P69B is also required for PC2-induced cell death, we transiently expressed PC2 and the PC2^{M3} fragment in WT and asP69B tomato plants. PC2 induced cell death was very weak in WT tomato plants. We therefore performed qRT-PCR to detect the induction of the early PTI tomato defense marker genes *SILrr22*, *SIPti5*, and *SIGras2* and HR marker gene *Sltprox1* as an alternative method (Rivas *et al.*, 2004; Nguyen *et al.*, 2010). We found that the tomato marker genes *SILrr22*, *SIPti5*, *SIGras2* and *Sltprox1* were up-regulated in response to PC2 expression, however, these genes were not induced in the *asP69B* tomato line (Fig. 6c). Interestingly, these genes were induced in both WT and asP69B tomatoes when these plants transiently expressed the PC2^{M3} mutant, providing further evidence that P69B participates in PC2 cleavage but not the perception of PC2 in tomato.

We also evaluated whether the cleavage process is important for PC2 triggered immunity in other plant species. Many *P69* homologs were present in the *N. benthamiana* and potato genomes, and constitute an expanded gene subfamily (Edgar, 2004; Letunic & Bork, 2019) (Fig. S10). In *N. benthamiana*, we found two *P69B* homologs (NbD047540.1 and NbD038132.1, Fig. S10). However, these proteases were not abundant or induced in apoplastic fluid (Grosse-Holz *et al.*, 2018).

NbD038072.1 (NbSBT5.2) has been reported as one of the most abundant extracellular proteases and functionally similar to tomato P69B (Paulus *et al.*, 2020). Therefore, we used VIGS to suppress the expression of *NbSBT5.2* in *N. benthamiana* (TRV: *SBT5.2*) and monitored PC2-induced cell death in the silenced plants. PC2-induced cell death was significantly weaker in TRV: *SBT5.2* plants when compared to TRV: *GFP* plants, but no difference was found with PC2^{M3} (Fig. S11a,b). Immunoblotting confirmed that PC2 was successfully expressed in *N. benthamiana* (Fig. S11c). These data suggest PC2 cleavage and elicited immunity in different plant species may require distinct proteases.

To further clarify that the cleavage process is important for PC2 triggered immunity, we generated a series of PC2 mutants and tested their function and *in vitro* cleavage by P69B. In comparison with PC2, the PC2^{M3} mutant (PC2¹³⁸⁻¹⁹⁸) triggered stronger cell death (Fig. 4a). Meanwhile, analysis of the *in vitro* cleavage result suggested that a ~10 kDa C-terminal PC2 fragment is released. Therefore, we reasoned that the cleavage site is likely present in a region between 100 to 138. Accordingly, we generated five PC2 mutants carrying large scale alanine substitutions in this region and only mutant PC2^{103-116A} was unable to induce cell death in *N. benthamiana* (with PC2^{116-126A} induced weak cell death)(Fig. 7a). Recent discoveries suggest that P69B is an aspartic acid-specific protease (Paulus *et al.*, 2020), we therefore individually mutated aspartic acid into alanine in the putative cleavage region. Neither the D105A nor D112A mutation led to clear cell death reduction. However, site-directed mutation of D117A significantly impaired PC2-induced cell death (Fig. 7b,c). Consistent with this observation, the mutant PC2^{D117A} is more abundant in planta and more resistant to P69B cleavage (Fig. 7d,e). These results further confirm that the PC2 cleavage process is critical for its function and that residue D117 is very likely essential for cleavage.

Serine protease inhibitors of *P. infestans* counteract PC2 cleavage

Earlier studies showed that *P. infestans* secretes Kazal-like protease inhibitor EPI1 and EPI1 homologs to repress P69B protease activity (Tian *et al.*, 2004; Tian *et al.*, 2005). In this study, we examined whether EPI inhibitors are able to suppress PC2-mediated plant immunity by directly preventing PC2 cleavage. We selected six *P. infestans* genes that encoding *EPI1*, *EPI2*, *EPI4*, *EPI6*, *EPI10*, and *EPI12*. We found that transient expression of EPI1, EPI4 or EPI10 suppressed PC2-induced cell death but had no impact on INF1- or XEG1- induced cell death, suggesting that EPI

inhibitors have a specific role in suppressing PC2-triggered cell death (Fig. 8a,b and S12a-d). These data are consistent with our earlier observation that the chemical inhibitor DCI inhibits only PC2-induced cell death but cannot inhibit INF1- or XEG1- mediated cell death (Fig. 5a).

To examine whether EPI1 suppression of PC2 depends on its inhibitory function, we utilized mutant EPI1^{P1}, an EPI1 mutant with the predicted active site P1 replaced with alanine (Tian *et al.*, 2004) (Fig. S13a). Transient expression in *N. benthamiana* illustrated that EPI1^{P1} was unable to repress PC2-mediated cell death. However, neither EPI1 nor EPI1^{P1} inhibited PC2^{M3}-induced cell death, indicating that the EPI1 inhibitor acts upstream of PC2^{M3} (Fig. S13b-d). EPI1 is composed of two Kazal-like domains, a four-cysteine atypical domain EPI1a, and a typical domain EPI1b (Tian & Kamoun, 2005). We cloned these two domains independently and tested their activity in repressing PC2-induced cell death. PC2-triggered cell death was inhibited by EPI1a but not by EPI1b (Fig. 8c,d). Neither EPI1a nor EPI1b repressed PC2^{M3} activity. This is in line with earlier reports indicating that EPI1a rather than EPI1b inhibits P69B protease activity.

We next examined whether the EPI1 protein could inhibit PC2 cleavage induced by P69B. Incubation of recombinant EPI1a with PC2 indicated that EPI1a inhibited PC2 cleavage in a concentration-dependent manner and this inhibition was not observed with the non-functional EPI1b fragment (Fig. 8e,f). These results confirm that subtilases play an important role in PC2 cleavage and that *P. infestans* protease inhibitors EPI1, EPI4, and EPI10 can block PC2 cleavage and PC2-induced cell death, depending on their inhibition activity.

Discussion

More than 20 years ago, tomato subtilisin-like protease P69B was identified as a PR protein that is rapidly induced at early infection by citrus viroid (Tornero *et al.*, 1996). P69B contains all the essential catalytic residues and is considered as an active protease that is involved in proteolytic defense in the plant extracellular matrix (Tornero *et al.*, 1997). Tian and colleagues demonstrated that P69B is a direct target of EPI1, a Kazal-like serine protease inhibitor from *P. infestans*, suggesting inhibition of P69B activity is important for pathogen colonization (Tian *et al.*, 2004). However, the role of P69B in plant defense has remained elusive. Here we provide biochemical evidence that P69B proteolytically cleaves *Phytophthora* apoplastic effector PC2. *In vivo* inhibition of P69B through the application of a chemical inhibitor or EPI1 suppresses PC2-triggered cell death (Fig. 5a, S13b,c). In

line with this observation, silencing of *P69B* in plants then prevents cleavage of PC2 impairs PC2 activated PR gene up-regulation (Fig. 6,c). All these data indicate that PC2 proteolytic cleavage by P69B is critical for PC2 triggered immunity. This is likely because the cleavage of PC2 releases a short bioactive peptide which can be recognized by plant PRRs. This is supported by the fact that PC2-triggered immunity in *N. benthamiana* requires BAK1, an important co-receptor for LRR-RK-type PRRs.

Plant proteases present a broad spectrum of biological functions. In this study, we showed that PC2 is targeted by the protease P69B. Tomato P69B paralogs such as P69A and P69D, contain all the catalytic residues but don't cleave PC2, suggesting the function of these family members is different. This could be due to gene duplication and subsequent neo-functionalization during evolution. To identify the substrates of P69B and paralogous proteases using biochemical approaches would help to fully understand the mode of action of these plant proteases. In general, plant proteases proteolytically cleave pathogen effectors to impair their biological functions and are considered important components of the defense response. Interestingly, a recent study of the *Ustilago* fungal protease inhibitor Pit2 demonstrated that pathogen utilizes plant extracellular protease to generate a powerful inhibitory peptide (Misas Villamil *et al.*, 2019). In another study, *Arabidopsis* aspartic proteases cleave the evolutionarily conserved bacterial protein MucD to inhibit bacterial pathogen growth as an antibacterial strategy (Wang *et al.*, 2019). Different from these discoveries, we showed here that extracellular cleavage of a *Phytophthora* effector PC2 by the plant protease P69B triggers immunity. This illustrates that plant extracellular proteases can be employed by both plants and their pathogens during co-evolution. Exploring the underlying mechanism is an important step to designing rational plant disease management strategies.

Studies of plant proteases in other pathosystems have indicated that proteases bind and preferentially cleave their substrate in a sequence context-dependent manner. It was recently shown that the P69A serine protease prefers to cleave after Asp (Reichardt *et al.*, 2018). More recently, tomato P69B was validated as an aspartic acid-specific protease (Paulus *et al.*, 2020). We developed a PC2 site-directed mutant PC2^{D117A} that was insensitive to P69B cleavage *in vitro*. Accordingly, this mutant also exhibited a weakened cell death phenotype. However, addition of excess P69B protease was still able to process the recombinant PC2^{D117A} protein, albeit at a reduced rate. We reason that the

P69B protease cleaves the selection substrates may not be sequence dependent only. Other factors such as modifications or conformation of the substrate may impact the specificity between P69B and its substrates. Western blot data revealed that PC2 has a larger molecular weight than anticipated, suggesting modifications of PC2 *in vivo* may exist. Future work will aim to capture the bioactive peptides that act as signals to induce defense responses.

Ortholog searches revealed PC2 orthologs present in a wide selection of oomycete species including downy mildew and *Salisapilia species*, although no homolog was found in *Albugo* species. In particular, PC2 orthologs are highly conserved across *Phytophthora* species and all *Phytophthora* PC2 proteins tested were able to trigger cell death in *N. benthamiana*. In contrast, the downy mildew ortholog, HpaPC2, was highly divergent in sequence from *Phytophthora* PC2 and was unable to induce cell death in *N. benthamiana*. Whether they activate immunity in their respective host plants remains to be determined. Interestingly, 16 of the 18 cysteines present in *Phytophthora* PC2 are conserved in other oomycete species and substitution of just two of these cysteines (C183A and C189A) was sufficient to abolish PC2 activity. This suggests these two residues may form a potential disulfide bond to maintain protein conformation. However, both cysteines are conserved between functional and non-functional PC2 orthologs. We reason that downy mildew PC2 homologs failed to trigger immunity due to sequence variations beyond these two residues. Nevertheless, it appears that PC2 is conserved across the oomycetes and that plants may have evolved immune machinery to specifically recognize this pathogen signal. However, obligate biotrophic pathogens may evade recognition through loss of function mutations such as deletion of the PC2 homolog in *Albugo* and gain of sequence polymorphisms as seen in downy mildew species. It was noted that PyuPC2 showed the smallest band size in the western blot while it has the longest amino acid sequence. One explanation could be the glycosylation of the PC2 protein in *N. benthamiana*. PC2 contains three potential N-glycosylation sites Asn-40 (NAT), Asn-95 (NAS) and Asn-135 (NCT), whereas PyuPC2 does not contain these sites. Whether glycosylation polymorphisms in PC2 orthologs play a role in triggering host immunity deserves further investigation in future.

To evade the plant surveillance system, *Phytophthora* may have evolved protease inhibitors such as the Kazal-like protease inhibitors (EPIs) to block PC2 extracellular processing. In order to validate whether EPI1 suppresses PC2-triggered defense to facilitate *P. infestans* infection, knocking out *EPI1*

would be advantageous. However, knocking out genes in *P. infestans* remains challenging. Regardless of the potential functional redundancy among EPI paralogs, it may not reveal a clear phenotype. Beside delivering protease inhibitor, *Phytophthora* may have evolved other strategies to counteract PC2-triggered immunity. For example, *Phytophthora* may secrete cytoplasmic effectors to block the secretion of proteases into the apoplast and indirectly block PC2-triggered immunity (Bozkurt *et al.*, 2011; Guo *et al.*, 2019).

Whether PC2 orthologs act as an effector or a MAMP during *Phytophthora* - host plant interaction is an interesting consideration. Our data demonstrated that PC2 induced cell death requires a PRR co-receptor, but not EDS1 and NDR1 in *N. benthamiana*. Furthermore, PC2 homologs are widely present in *S. sapeloensis*, a non-pathogenic oomycete species. These data tend to suggest that PC2 may act more like a MAMP. Revealing the working mechanism of plant immunity to MAMPs provides solutions to enhance plant resistance. Whether PC2 plays a biological role during infection remains unknown. In this study, we were unable to knockout *PsPC2* in *P. sojae* by CRISPR/Cas9, suggesting PC2 may have a basic biological function that deserves further exploration. PC2 triggers cell death in several *Solanum* plants such as *N. benthamiana*, *N. tabacum*, *S. lycopersicum*, and *S. tuberosum*. Meanwhile, P69 homologs are present in an array of *Solanum* genomes. We therefore hypothesize that plant evolved PRRs recognizing PC2, and the recognition pathway may be conserved across *Solanaceae* species. This implies that the plant PRRs recognizing PC2 could be valuable in agricultural applications. Indeed, emerging studies reveal that genetic manipulation of plant PRRs recognizing pathogen extracellular effectors such as elicitor, NLP, XEG1, enhance basal resistance to *Phytophthora* (Albert *et al.*, 2015; Wang *et al.*, 2018). Cloning of the specific PRR gene and functional allele screen may provide a resource to engineering durable plant resistance to *Phytophthora*.

Acknowledgments

We are grateful for help from Prof. Sophien Kamoun, Sylvain Raffaele, Abbas Maqbool, Jiorgos Kourelis, Chih-Hang Wu and Liliana M. Cano (The Sainsbury Laboratory) and all the lab members in Dong's group in NJAU. Prof. Wenbo Ma (UCR), Prof. Gunther Doehlemann (Univ. Cologne) and Prof. Cyril Zipfel (Univ. of Zurich and Univ. East Anglia) are appreciated for helpful suggestions. We

thank Prof. Chuanyou Li (CAS) for offering plant materials. This study is also supported by the high-performance computing platform of Bioinformatics Center, Nanjing Agricultural University. This work is supported by the National Natural Science Foundation of China (31772144, 31721004), the Fok Ying-Tong Education Foundation (151025), Fundamental Research Funds for Central Universities (JCQY201904, KYXK202010), ERC Consolidator Grant 616449 and BBSRC grant BB/S003193/1. S. Wang received support from the Postgraduate Research & Practice Innovation Program of Jiangsu Province (KYCX17_0579).

Author contributions

S.W., R.X., S.F., J.K.P., M.S., J.H., J.W. and S.D. performed experiments; H.S., Yan Wang, V.V. and D.G.O.S. analyzed data; S.W., Yuanchao Wang, X.Z., R.A.L.vdH. and S.D. designed experiments; S.W., Yan Wang and S.D. wrote the manuscript.

References

- Ah-Fong AMV, Shrivastava J, Judelson HS. 2017. Lifestyle, gene gain and loss, and transcriptional remodeling cause divergence in the transcriptomes of *Phytophthora infestans* and *Pythium ultimum* during potato tuber colonization. *BMC Genomics* **18**(1): 764.
- Albert I, Bohm H, Albert M, Feiler CE, Imkampe J, Wallmeroth N, Brancato C, Raaymakers TM, Oome S, Zhang H, et al. 2015. An RLP23-SOBIR1-BAK1 complex mediates NLP-triggered immunity. *Nat Plants* **1**: 15140.
- Armstrong MR, Whisson SC, Pritchard L, Bos JIB, Venter E, Avrova AO, Rehmany AP, Böhme U, Brooks K, Cherevach I, et al. 2005. An ancestral oomycete locus contains late blight avirulence gene *Avr3a*, encoding a protein that is recognized in the host cytoplasm. *Proc Natl Acad Sci U S A* **102**(21): 7766-7771.
- Boller T, He SY. 2009. Innate immunity in plants: an arms race between pattern recognition receptors in plants and effectors in microbial pathogens. *Science* **324**(5928): 742-744.
- Bozkurt TO, Schornack S, Win J, Shindo T, Ilyas M, Oliva R, Cano LM, Jones AME, Huitema E, van der Hoorn RAL, et al. 2011. *Phytophthora infestans* effector AVRblb2 prevents secretion of a plant immune protease at the haustorial interface. *Proc Natl Acad Sci U S A* **108**(51): 20832-20837.
- Chen H, Shu H, Wang L, Zhang F, Li X, Ochola SO, Mao F, Ma H, Ye W, Gu T, et al. 2018. *Phytophthora methylomes* are modulated by 6mA methyltransferases and associated with adaptive genome regions. *Genome Biol* **19**(1): 181.
- Clark K, Franco JY, Schwizer S, Pang Z, Hawara E, Liebrand TWH, Pagliaccia D, Zeng L, Gurung FB, Wang P, et al. 2018. An effector from the Huanglongbing-associated pathogen targets citrus proteases. *Nat Commun* **9**(1): 1718.
- de Wit PJGM, Spikman G. 1982. Evidence for the occurrence of race and cultivar-specific elicitors of necrosis

in intercellular fluids of compatible interactions of *Cladosporium fulvum* and tomato. *Physiological Plant Pathology* **21**(1): 1-11.

Dong S, Stam R, Cano LM, Song J, Sklenar J, Yoshida K, Bozkurt TO, Oliva R, Liu Z, Tian M, et al. 2014. Effector specialization in a lineage of the Irish potato famine pathogen. *Science (New York, N.Y.)* **343**(6170): 552-555.

Du Y, Stegmann M, Misas Villamil JC. 2016. The apoplast as battleground for plant-microbe interactions. *New Phytol.* **209**(1): 34-38.

Edgar RC. 2004. MUSCLE: multiple sequence alignment with high accuracy and high throughput. *Nucleic Acids Research* **32**(5): 1792-1797.

Gijzen M, Nurnberger T. 2006. Nep1-like proteins from plant pathogens: recruitment and diversification of the NPP1 domain across taxa. *Phytochemistry* **67**(16): 1800-1807.

Grosse-Holz F, Kelly S, Blaskowski S, Kaschani F, Kaiser M, van der Hoorn RAL. 2018. The transcriptome, extracellular proteome and active secretome of agroinfiltrated *Nicotiana benthamiana* uncover a large, diverse protease repertoire. *Plant biotechnology journal* **16**(5): 1068-1084.

Guo B, Wang H, Yang B, Jiang W, Jing M, Li H, Xia Y, Xu Y, Hu Q, Wang F, et al. 2019. *Phytophthora sojae* Effector PsAvh240 Inhibits Host Aspartic Protease Secretion to Promote Infection. *Molecular plant* **12**(4): 552-564.

Haas BJ, Kamoun S, Zody MC, Jiang RH, Handsaker RE, Cano LM, Grabherr M, Kodira CD, Raffaele S, Torto-Alalibo T, et al. 2009. Genome sequence and analysis of the Irish potato famine pathogen *Phytophthora infestans*. *Nature* **461**(7262): 393-398.

Heese A, Hann DR, Gimenez-Ibanez S, Jones AM, He K, Li J, Schroeder JI, Peck SC, Rathjen JP. 2007. The receptor-like kinase SERK3/BAK1 is a central regulator of innate immunity in plants. *Proc Natl Acad Sci U S A* **104**(29): 12217-12222.

-
- Huang J, Chen L, Lu X, Peng Q, Zhang Y, Yang J, Zhang BY, Yang B, Waletich JR, Yin W, et al. 2019. Natural allelic variations provide insights into host adaptation of *Phytophthora* avirulence effector PsAvr3c. *New Phytol* **221**(2): 1010-1022.
- Ilyas M, Horger AC, Bozkurt TO, van den Burg HA, Kaschani F, Kaiser M, Belhaj K, Smoker M, Joosten MH, Kamoun S, et al. 2015. Functional Divergence of Two Secreted Immune Proteases of Tomato. *Curr Biol* **25**(17): 2300-2306.
- Jones JD, Dangl JL. 2006. The plant immune system. *Nature* **444**(7117): 323-329.
- Kamoun S, van West P, de Jong AJ, de Groot KE, Vleeshouwers VG, Govers F. 1997. A gene encoding a protein elicitor of *Phytophthora infestans* is down-regulated during infection of potato. *Mol. Plant Microbe Interact.* **10**(1): 13-20.
- Kaschani F, Shabab M, Bozkurt T, Shindo T, Schornack S, Gu C, Ilyas M, Win J, Kamoun S, van der Hoorn RA. 2010. An effector-targeted protease contributes to defense against *Phytophthora infestans* and is under diversifying selection in natural hosts. *Plant Physiol* **154**(4): 1794-1804.
- Kavroulakis N, Papadopoulou KK, Ntougias S, Zervakis GI, Ehaliotis C. 2006. Cytological and other aspects of pathogenesis-related gene expression in tomato plants grown on a suppressive compost. *Annals of botany* **98**(3): 555-564.
- Krüger J, Thomas CM, Golstein C, Dixon MS, Smoker M, Tang S, Mulder L, Jones JD. 2002. A tomato cysteine protease required for Cf-2-dependent disease resistance and suppression of autonecrosis. *Science* **296**(5568): 744-747.
- Letunic I, Bork P. 2019. Interactive Tree Of Life (iTOL) v4: recent updates and new developments. *Nucleic Acids Research* **47**(W1): W256-W259.
- Liebrand TW, van den Berg GC, Zhang Z, Smit P, Cordewener JH, America AH, America AH, Sklenar J, Jones AM, Tameling WI, et al. 2013. Receptor-like kinase SOBIR1/EVR interacts with receptor-like proteins in

plant immunity against fungal infection. *Proc. Natl. Acad. Sci. U.S.A.* **110**(24): 10010-10015.

Liu Y, Patricelli MP, Cravatt BF. 1999. Activity-based protein profiling: The serine hydrolases. *Proc Natl Acad Sci U S A* **96**(26): 14694-14699.

Liu Z, Bos JI, Armstrong M, Whisson SC, da Cunha L, Torto-Alalibo T, Win J, Avrova AO, Wright F, Birch PR, et al. 2005. Patterns of diversifying selection in the phytotoxin-like *scr74* gene family of *Phytophthora infestans*. *Mol Biol Evol* **22**(3): 659-672.

Ma Z, Song T, Zhu L, Ye W, Wang Y, Shao Y, Dong S, Zhang Z, Dou D, Zheng X, et al. 2015. A *Phytophthora sojae* Glycoside Hydrolase 12 Protein Is a Major Virulence Factor during Soybean Infection and Is Recognized as a PAMP. *Plant Cell* **27**(7): 2057-2072.

Miao S, Liu J, Guo J, Li JF. 2019. Engineering plants to secrete affinity-tagged pathogen elicitors for deciphering immune receptor complex or inducing enhanced immunity. *J Integr Plant Biol* **62**(6): 761-776.

Misas Villamil JC, Mueller AN, Demir F, Meyer U, Okmen B, Schulze Huynck J, Breuer M, Dauben H, Win J, Huesgen PF, et al. 2019. A fungal substrate mimicking molecule suppresses plant immunity via an inter-kingdom conserved motif. *Nat Commun* **10**(1): 1576.

Mueller AN, Ziemann S, Treitschke S, Assmann D, Doehlemann G. 2013. Compatibility in the *Ustilago maydis*-maize interaction requires inhibition of host cysteine proteases by the fungal effector Pit2. *PLoS Pathog* **9**(2): e1003177.

Newman MA, Sundelin T, Nielsen JT, Erbs G. 2013. MAMP (microbe-associated molecular pattern) triggered immunity in plants. *Front Plant Sci* **4**: 139.

Nguyen HP, Chakravarthy S, Velásquez AC, McLane HL, Zeng L, Nakayashiki H, Park D-H, Collmer A, Martin GB. 2010. Methods to study PAMP-triggered immunity using tomato and *Nicotiana benthamiana*. *Molecular plant-microbe interactions : MPMI* **23**(8): 991-999.

-
- Norero NS, Castellote MA, de la Canal L, Feingold SE. 2016. Genome-Wide Analyses of Subtilisin-Like Serine Proteases on *Solanum tuberosum*. *American Journal of Potato Research* **93**(5): 485-496.
- Orsomando G, Lorenzi M, Raffaelli N, Dalla Rizza M, Mezzetti B, Ruggieri S. 2001. Phytotoxic protein PcF, purification, characterization, and cDNA sequencing of a novel hydroxyproline-containing factor secreted by the strawberry pathogen *Phytophthora cactorum*. *J. Biol. Chem.* **276**(24): 21578-21584.
- Panda A, Sen D, Ghosh A, Gupta A, C MM, Prakash Mishra G, Singh D, Ye W, Tyler BM, Tripathy S. 2018. EumicrobeDBLite: a lightweight genomic resource and analytic platform for draft oomycete genomes. *Molecular plant pathology* **19**(1): 227-237.
- Paulus JK, Kourelis J, Ramasubramanian S, Homma F, Godson A, Hörger AC, Hong TN, Krahn D, Ossorio Carballo L, Wang S, et al. 2020. Extracellular proteolytic cascade in tomato activates immune protease Rcr3. *Proc Natl Acad Sci U S A* **117**(29): 17409-17417.
- Pogorelko GV, Juvalé PS, Rutter WB, Hutten M, Maier TR, Hewezi T, Paulus J, van der Hoorn RA, Grundler FM, Siddique S, et al. 2019. Re-targeting of a plant defense protease by a cyst nematode effector. *Plant J* **98**(6): 1000-1014.
- Raffaele S, Farrer RA, Cano LM, Studholme DJ, MacLean D, Thines M, Jiang RH, Zody MC, Kunjeti SG, Donofrio NM, et al. 2010. Genome evolution following host jumps in the Irish potato famine pathogen lineage. *Science* **330**(6010): 1540-1543.
- Raffaele S, Win J, Cano LM, Kamoun S. 2010. Analyses of genome architecture and gene expression reveal novel candidate virulence factors in the secretome of *Phytophthora infestans*. *BMC Genomics* **11**(1): 637.
- Reichardt S, Repper D, Tuzhikov AI, Galiullina RA, Planas-Marques M, Chichkova NV, Vartapetian AB, Stintzi A, Schaller A. 2018. The tomato subtilase family includes several cell death-related proteinases with caspase specificity. *Sci Rep* **8**(1): 10531.

-
- Rivas S, Rougon-Cardoso A, Smoker M, Schauser L, Yoshioka H, Jones JD. 2004. CITRX thioredoxin interacts with the tomato Cf-9 resistance protein and negatively regulates defence. *Embo j.* **23**(10): 2156-2165.
- Rooney HC, Van't Klooster JW, van der Hoorn RA, Joosten MH, Jones JD, de Wit PJ. 2005. *Cladosporium* Avr2 inhibits tomato Rcr3 protease required for Cf-2-dependent disease resistance. *Science* **308**(5729): 1783-1786.
- Saunders DG, Win J, Cano LM, Szabo LJ, Kamoun S, Raffaele S. 2012. Using hierarchical clustering of secreted protein families to classify and rank candidate effectors of rust fungi. *PLoS One* **7**(1): e29847.
- Song T, Ma Z, Shen D, Li Q, Li W, Su L, Ye T, Zhang M, Wang Y, Dou D. 2015. An Oomycete CRN Effector Reprograms Expression of Plant *HSP* Genes by Targeting their Promoters. *PLoS Pathog* **11**(12): e1005348.
- Sonnhammer EL, Eddy SR, Durbin R. 1997. Pfam: a comprehensive database of protein domain families based on seed alignments. *Proteins* **28**(3): 405-420.
- Stergiopoulos I, de Wit PJGM. 2009. Fungal Effector Proteins. *Annual Review of Phytopathology* **47**(1): 233-263.
- Sueldo D, Ahmed A, Misas-Villamil J, Colby T, Tameling W, Joosten MH, van der Hoorn RA. 2014. Dynamic hydrolase activities precede hypersensitive tissue collapse in tomato seedlings. *New Phytol* **203**(3): 913-925.
- Templeton MD, Raaymakers TM, Baillieux F. 1994. Small, Cysteine-Rich proteins and Recognition in Fungal-Plant Interactions. *Mol Plant Microbe Interact* **7**(3): 320-325.
- Tian M, Benedetti B, Kamoun S. 2005. A Second Kazal-like protease inhibitor from *Phytophthora infestans* inhibits and interacts with the apoplastic pathogenesis-related protease P69B of tomato. *Plant Physiol* **138**(3): 1785-1793.

-
- Tian M, Huitema E, Da Cunha L, Torto-Alalibo T, Kamoun S. 2004. A Kazal-like extracellular serine protease inhibitor from *Phytophthora infestans* targets the tomato pathogenesis-related protease P69B. *J Biol Chem* **279**(25): 26370-26377.
- Tian M, Kamoun S. 2005. A two disulfide bridge Kazal domain from *Phytophthora* exhibits stable inhibitory activity against serine proteases of the subtilisin family. *BMC Biochem* **6**: 15.
- Tornero P, Conejero V, Vera P. 1996. Primary structure and expression of a pathogen-induced protease (PR-P69) in tomato plants: Similarity of functional domains to subtilisin-like endoproteases. *Proc. Natl. Acad. Sci. U.S.A.* **93**(13): 6332-6337.
- Tornero P, Conejero V, Vera P. 1997. Identification of a new pathogen-induced member of the subtilisin-like processing protease family from plants. *J. Biol. Chem.* **272**(22): 14412-14419.
- Torto TA, Li S, Styer A, Huitema E, Testa A, Gow NA, van West P, Kamoun S. 2003. EST mining and functional expression assays identify extracellular effector proteins from the plant pathogen *Phytophthora*. *Genome Res.* **13**(7): 1675-1685.
- Wang Y, Garrido-Oter R, Wu J, Winkelmuller TM, Agler M, Colby T, Nobori T, Kemen E, Tsuda K. 2019. Site-specific cleavage of bacterial MucD by secreted proteases mediates antibacterial resistance in *Arabidopsis*. *Nat Commun* **10**(1): 2853.
- Wang Y, Wang Y, Wang Y. 2020. Apoplastic Proteases: Powerful Weapons against Pathogen Infection in Plants. *Plant Communications* **1**(4): 100085.
- Wang Y, Xu Y, Sun Y, Wang H, Qi J, Wan B, Ye W, Lin Y, Shao Y, Dong S, et al. 2018. Leucine-rich repeat receptor-like gene screen reveals that *Nicotiana* RXEG1 regulates glycoside hydrolase 12 MAMP detection. *Nat Commun* **9**(1): 594.
- Ziemann S, van der Linde K, Lahrmann U, Acar B, Kaschani F, Colby T, Kaiser M, Ding Y, Schmelz E, Huffaker A, et al. 2018. An apoplastic peptide activates salicylic acid signalling in maize. *Nat Plants* **4**(3): 172-180.

Figure legends

Fig. 1 Screening of *Phytophthora infestans* SCR proteins led to the discovery of PC2. (a) Screening pipeline for small cysteine rich proteins from *P. infestans*. (b) to (c) Three candidate SCR proteins triggered cell death in *Nicotiana benthamiana*. (b) Representative *N. benthamiana* leaves 5 days post inoculation with *Agrobacterium* strains expressing SCR effectors. (c) Quantitative fluorescence intensity of cell death. Means \pm SE from three independent replicates are shown. Asterisks indicate significant differences (* $P < 0.05$; ** $P < 0.01$; *** $P < 0.001$; one-way ANOVA).

Fig. 2 PC2 induced plant immune response. (a) to (b) PC2-induce cell death in *Nicotiana benthamiana* and the C-terminal tags don't influence function. (a) Representative *N. benthamiana* leaves 5 d post-inoculation with *Agrobacterium* strains expressing PC2, PC2-His, or PC2-HA cloned in PVX vector, along with EV. INF1-HA was used as a positive control. (b) Quantitative fluorescence intensity of cell death. Means \pm SE from three independent replicates are shown. Asterisks indicate significant differences (*** $P < 0.001$; one-way ANOVA). (c) to (d) Reactive oxygen species (ROS) accumulation at 2.5 dpi in *N. benthamiana* leaves infiltrated with agrobacteria containing PC2, PC2-His, PC2-HA, or EV, as detected by DAB staining. (c) Representative photographs. (d) Quantitative intensity of DAB staining. Means \pm SE from three independent replicates are shown. Asterisks indicate significant differences (*** $P < 0.001$; one-way ANOVA). (e) Transcript level of *PR1* and *RbohB* induced by PC2 in *N. benthamiana* leaves. The gene expression was examined at different time points by using qRT-PCR. Means \pm SE from three independent replicates are shown. (f) to (g) PC2-induced cell death in *N. benthamiana* leaves was inhibited by DPI and LaCl_3 . (f) Representative photographs. Each inhibitor was infiltrated into *N. benthamiana* leaves 6 hours before PC2 agroinfiltration and the leaves were photographed 5 days later. (g) Quantitative fluorescence intensity of cell death. Means \pm SE from five independent replicates are shown. Asterisks indicate significant differences (* $P < 0.05$; *** $P < 0.001$; one-way ANOVA). (h) to (i) BAK1 is required for PC2-triggered cell death in *N. benthamiana*. (h) *N. benthamiana* plants were subjected to VIGS by inoculation with TRV constructs (TRV: *GFP*, TRV: *BAK1*, and TRV: *SOBIR1*). Four weeks after inoculation, PC2

was transiently expressed in the gene-silenced leaves and then leaves were photographed 5 days later.

(i) Quantitative fluorescence intensity of cell death. Means \pm SE from five independent replicates are shown. Asterisks indicate significant differences (***) $P < 0.001$; one-way ANOVA).

Fig. 3 PC2 homologs are widely present in oomycete species. (a) Phylogeny of PC2 from selected species. The tree was constructed by the neighbour-joining (NJ) algorithm implemented in MEGA7. Bootstrap percentage support for each branch is indicated. The scale bar represents 10% weighted sequence divergence. “+”, cell death induction in *Nicotiana benthamiana*; “-”, no cell death induction in *N. benthamiana*; “ND”, not determined. (b) to (c) PC2 homologs from *Phytophthora sojae* (PsPC2-HA) and *Peronophythora litchii* (PIPC2-HA) induced cell death in *N. benthamiana*. (b) Representative *N. benthamiana* leaves 5 days post-infiltration with *Agrobacterium* strains expressing PC2 homologs. (c) Quantification of the fluorescence intensity induced by PC2 homologs. The fluorescence intensity induced by PC2 was assigned the value 1.0. Means \pm SE from five independent replicates are shown. (d) Immunoblot analysis of PC2 or homologs fused with HA tags transiently expressed in *N. benthamiana* leaves.

Fig. 4 PC2 protein sequence signatures that are required for cell death. (a) to (b) PC2^{M3}, a functional peptide that induce cell death. (a) Various PC2 mutants were constructed according to PC2 and HpaPC2 functional differentiation. Pictures were taken 5 days after infiltration with *Agrobacterium* strains carrying a series of mutants. (b) Quantification of the fluorescence intensity induced by different mutants in *Nicotiana benthamiana* leaves. The fluorescence intensity induced by PC2 was assigned the value 1.0. Means \pm SE from five independent replicates are shown. (c) Immunoblot analysis of PC2 mutants fused with HA tags transiently expressed in *N. benthamiana* leaves.

Fig. 5 Plant subtilase P69B cleaves PC2 protein. (a) to (b) PC2-induced cell death in *Nicotiana benthamiana* leaves was inhibited by plant protease inhibitor cocktail and serine protease inhibitor DCI. (a) Representative photographs. The *N. benthamiana* leaves were infiltrated with the cocktail

and E-64 6 hours before agrobacterium-injected PC2, or DCI 12 hours after PC2 expression. E-64, a cysteine protease inhibitor, used as a control. (b) Quantification of PC2-induced fluorescence intensity in *N. benthamiana* leaves after treatment by chemical inhibitors. Fluorescence intensity triggered by PC2 under respective buffer treatment was assigned the value 1.0. Means \pm SE from six independent replicates are shown. Asterisks indicate significant differences (** $P < 0.01$; *** $P < 0.001$; one-way ANOVA). (c) DCI inhibits serine protease activity in tomato (*Solanum lycopersicum*) and *N. benthamiana* apoplastic fluids. The apoplastic fluids were incubated for 30 min with DCI. E-64 was used as a control. Active serine proteases were labelled using FP-Tamra. Labelled proteins were detected in a protein gel by fluorescent scanning. (d) The PC2 protein was cleaved by P69B *in vitro*. HA-tagged P69B or homologs were expressed in *N. benthamiana*, and FLAG-PC2-His protein was expressed in *E. coli*. PC2 and P69B or its homologs protein were co-incubated at 10°C for 30 minutes. The small band indicated PC2 cleavage products and were detected using anti-FLAG immunoblot. (e) to (f) Cleavage of PC2 was gradually increased after adding the various concentrations of P69B or the incubation time. (e) Representative photographs. (f) Quantification of the PC2 and small PC2 signals after incubation with P69B. Signals were quantified from Western blots with ImageJ. Means \pm SE from three independent replicates are shown. (g) to (h) Serine protease inhibitor DCI prevented P69B cleavage of PC2 protein. (g) Representative photographs. HA-tagged P69B protein was added into the tube after FLAG-tagged PC2 protein and DCI were co-incubate in 4°C for 30 minutes. The cleavage products were gradually reduced in the presence of 0.5 mM, 1 mM, and 2 mM DCI (according concentrations for DMSO are 3.5 mM, 7 mM, and 14 mM). The cleavage products were detected using anti-FLAG immunoblot. (h) Quantification of the small PC2 signals after different treatments. Signals were quantified from Western blots with ImageJ. Means \pm SE from three independent replicates are shown.

Fig. 6 Plant subtilase P69B is required for PC2-triggered immunity. (a) The *P69B* expression level in asP69B tomato determined by qRT-PCR. The P69B silenced transgenic tomato line (asP69B) was generated in the Money Maker (MM-Cf0, WT) background (Paulus *et al.*, 2020). Actin was used as an endogenous reference for normalization. Means \pm SE from three independent replicates are shown. Asterisks indicate significant differences (*** $P < 0.001$; one-way ANOVA). (b) Apoplastic

fluid extracted from asP69B did not cleave PC2 protein. PC2 recombinant protein was co-incubated with the apoplastic fluids (AF) extracted from WT or asP69B tomato plants. Cleavage products were detected using anti-FLAG immunoblot. (c) PC2, not PC2^{M3}, induced up-regulation of tomato defense-related genes were impaired in asP69B plants. The gene expression was examined by qRT-PCR. Actin was used as an endogenous reference for normalization. The expression changes of *SILrr22*, *SIPti5* and *SIGras2* genes were detected 12 hours after PC2 expression and *SltpoxC1* is the result of 48 hours after PC2 expression. Means \pm SE from three independent replicates are shown. Asterisks indicate significant differences (* $P < 0.05$; ** $P < 0.01$; *** $P < 0.001$; one-way ANOVA).

Fig. 7 Screen PC2 mutants that are resistant to P69B protease cleavage. (a) Mutant PC2^{103-116A} cannot induce cell death in *Nicotiana benthamiana*. A total of five mutants covering 46 amino acids from 103-148 are generated based on PC2 fragment. The numbers refer that all the residues in this region are substituted by alanine. All tested mutants were transiently expressed in *N. benthamiana* leaves by agroinfiltration. (b) to (c) PC2^{D117A} induce weakened cell death in *N. benthamiana*. (b) Representative photographs. Three mutants PC2^{D105A}, PC2^{D112A} and PC2^{D117A} that substituted the Asp to Ala residues in or around 103-116 region were created. All tested mutants were transiently expressed in *N. benthamiana* leaves by agroinfiltration. (c) Quantification of the fluorescence intensity induced by different mutants in *N. benthamiana* leaves. The fluorescence intensity induced by PC2 was assigned the value 1.0. Means \pm SE from three independent replicates are shown. Asterisks indicate significant differences (* $P < 0.05$; ** $P < 0.01$; one-way ANOVA). (d) Immunoblot analysis of PC2 mutants fused with HA tag transiently expressed in *N. benthamiana* leaves. (e) PC2^{D117A} significantly reduced the cleavage under the P69B treatment. PC2 or the mutants' recombinant protein were co-incubated with purified P69B protein extracted from *N. benthamiana* leaves. Cleavage products were detected using anti-FLAG immunoblot.

Fig. 8 Serine protease inhibitors secreted by *Phytophthora infestans* counteract PC2 cleavage. (a) to (b) PC2 induced cell death in *Nicotiana benthamiana* leaves was inhibited by *P. infestans* secreted serine protease inhibitor EPI1, EPI4 and EPI10. (a) Representative photographs. The *N. benthamiana*

leaves were infiltrated with different EPIs 36 hours before PC2 expression. (b) Quantification of fluorescence intensity induced by PC2 in *N. benthamiana* leaves under different EPIs treatment. The PC2-elicited fluorescence with EV treatment was assigned the value 1.0. Means \pm SE from six independent replicates are shown. Asterisks indicate significant differences (** $P < 0.01$; one-way ANOVA). (c) to (d) Cell death induced by PC2, not PC2^{M3}, was inhibited by EPI1a. (c) Representative photographs. The *N. benthamiana* leaves were infiltrated with the EPI1a and EPI1b 36 hours before PC2 expression. (d) Quantification of fluorescence intensity induced by PC2 in *N. benthamiana* leaves after EPI1a treatment. The PC2-elicited fluorescence with EV treatment was assigned the value 1.0. Means \pm SE from six independent replicates are shown. Asterisk indicates significant differences (** $P < 0.01$; one-way ANOVA). (e) to (f) Recombinant EPI1a inhibits P69B cleavage of PC2 protein. (e) Representative photographs. FLAG-EPI1a and FLAG-EPI1b recombinant protein were expressed in *E. coli*. After the preincubation of P69B with EPI1a or EPI1b, PC2 protein was added into tubes. PC2 were gradually reduced in the presence of 0.5, 2.5, or 12.5 μ M purified EPI1a protein. EPI1b, a non-functional Kazal-like domain, served as a control. (f) Quantification of the small PC2 signals after different treatments. Signals were quantified from Western blots with ImageJ. Means \pm SE from three independent replicates are shown.

Supporting information

Fig. S1 Melting curves analysis of the qRT-PCR used in this study.

Fig. S2 Screening of *P. infestans* SCR proteins led to the discovery of PC2.

Fig. S3 PC2 is up-regulated during infection and peaks at 48 hours post infection.

Fig. S4 *Solanum* plants infiltrated with PC2 showed symptoms of cell death or necrosis.

Fig. S5 BAK1 is required for PC2-triggered cell death in *N. benthamiana*.

Fig. S6 PC2-induced cell death requires *SGT1*, but not *EDS1*, *NDR1* and *RAR1*.

Fig. S7 Amino acid sequence alignment of PC2 family effectors.

Fig. S8 Site-directed mutagenesis revealed that cysteines at 183 and 189 positions are required for PC2^{M3}-induced cell death.

Fig. S9 The other protease inhibitors we tested in this study don't suppress PC2-induced cell death.

Fig. S10 Phylogeny of subtilases of tomato, potato and *N. benthamiana*.

Fig. S11 A distantly related SBT in *N. benthamiana* participates in PC2-triggered immune response.

Fig. S12 The *P. infestans* secreted Kazal-like serine protease inhibitors cannot suppress INF1 and XEG1 induced cell death.

Fig. S13 Kazal-like serine protease inhibitor EPI1 suppresses PC2-induced cell death.

Table S1 Annotation of predicted secreted proteins from *P. infestans*.

Table S2 Putative SCR secreted proteins identified in this study.

Table S3 PC2 and its orthologs in oomycete species.

Table S4 Plasmid constructs used in the study.

Table S5 Primers used in this study.

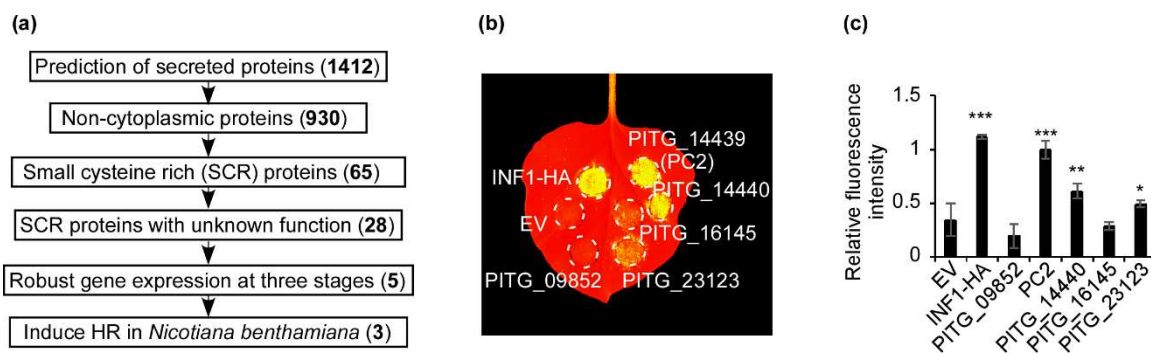


Fig. 1 Screening of *P. infestans* SCR proteins led to the discovery of PC2. (a) Screening pipeline for small cysteine rich proteins from *P. infestans*. (b) to (c) Three candidate SCR proteins triggered cell death in *N. benthamiana*. (b) Representative *N. benthamiana* leaves 5 days post inoculation with *Agrobacterium* strains expressing SCR effectors. (c) Quantitative fluorescence intensity of cell death. Means \pm SE from three independent replicates are shown. Asterisks indicate significant differences (* $P < 0.05$; ** $P < 0.01$; *** $P < 0.001$; one-way ANOVA).

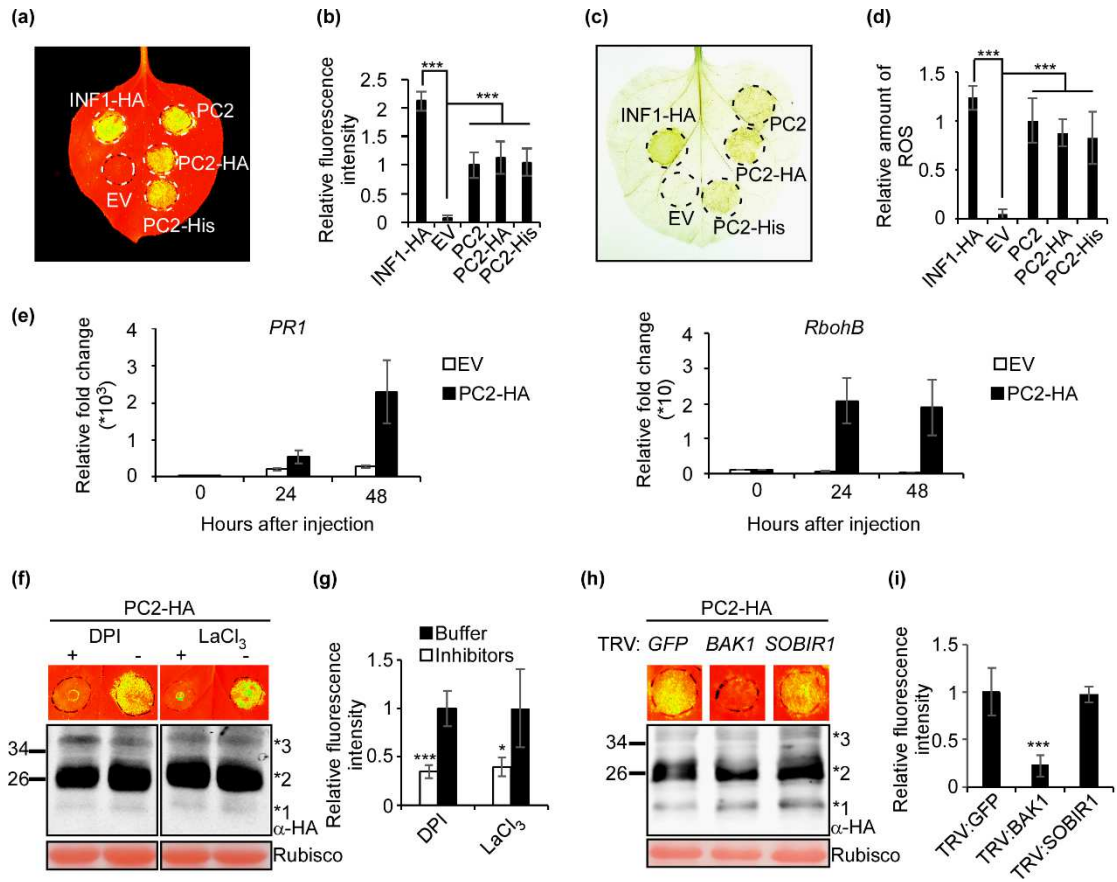


Fig. 2 PC2 induced plant immune response. (a) to (b) PC2-induce cell death in *N. benthamiana* and the C-terminal tags don't influence function. (a) Representative *N. benthamiana* leaves 5 d post-inoculation with *Agrobacterium* strains expressing PC2, PC2-His, or PC2-HA cloned in PVX vector, along with EV. INF1-HA was used as a positive control. (b) Quantitative fluorescence intensity of cell death. Means \pm SE from three independent replicates are shown. Asterisks indicate significant differences (**P< 0.01; ***P< 0.001; one-way ANOVA). (c) to (d) ROS accumulation at 2.5 dpi in *N. benthamiana* leaves infiltrated with agrobacteria containing PC2, PC2-His, PC2-HA, or EV, as detected by DAB staining. (c) Representative photographs. (d) Quantitative intensity of DAB staining. Means \pm SE from three independent replicates are shown. Asterisks indicate significant differences (**P< 0.01; ***P< 0.001; one-way ANOVA). (e) Transcript level of *PR1* and *RbohB* induced by PC2 in *N. benthamiana* leaves. The gene expression was examined at different time points by using qRT-PCR. Means \pm SE from three independent replicates are shown. (f) to (g) PC2-induced cell death in *N. benthamiana* leaves was inhibited by DPI and LaCl₃. (f) Representative photographs. Each inhibitor was infiltrated into *N. benthamiana* leaves 6 hours before PC2 agroinfiltration and the leaves were photographed 5 days later. (g) Quantitative fluorescence intensity of cell death. Means \pm SE from five independent replicates are shown. Asterisks indicate significant differences (*P<0.05; **P< 0.01; ***P< 0.001; one-way ANOVA). (h) to (i) BAK1 is required for PC2-triggered cell death in *N. benthamiana*. (h) *N. benthamiana* plants were subjected to VIGS by inoculation with TRV constructs (TRV: *GFP*, TRV: *BAK1*, and TRV: *SOBIR1*). Four weeks after inoculation, PC2 was transiently expressed in the gene-silenced leaves and then leaves were photographed 5 days later. (i) Quantitative fluorescence intensity of cell death. Means \pm SE from five independent replicates are shown. Asterisks indicate significant differences (**P< 0.01; ***P< 0.001; one-way ANOVA).

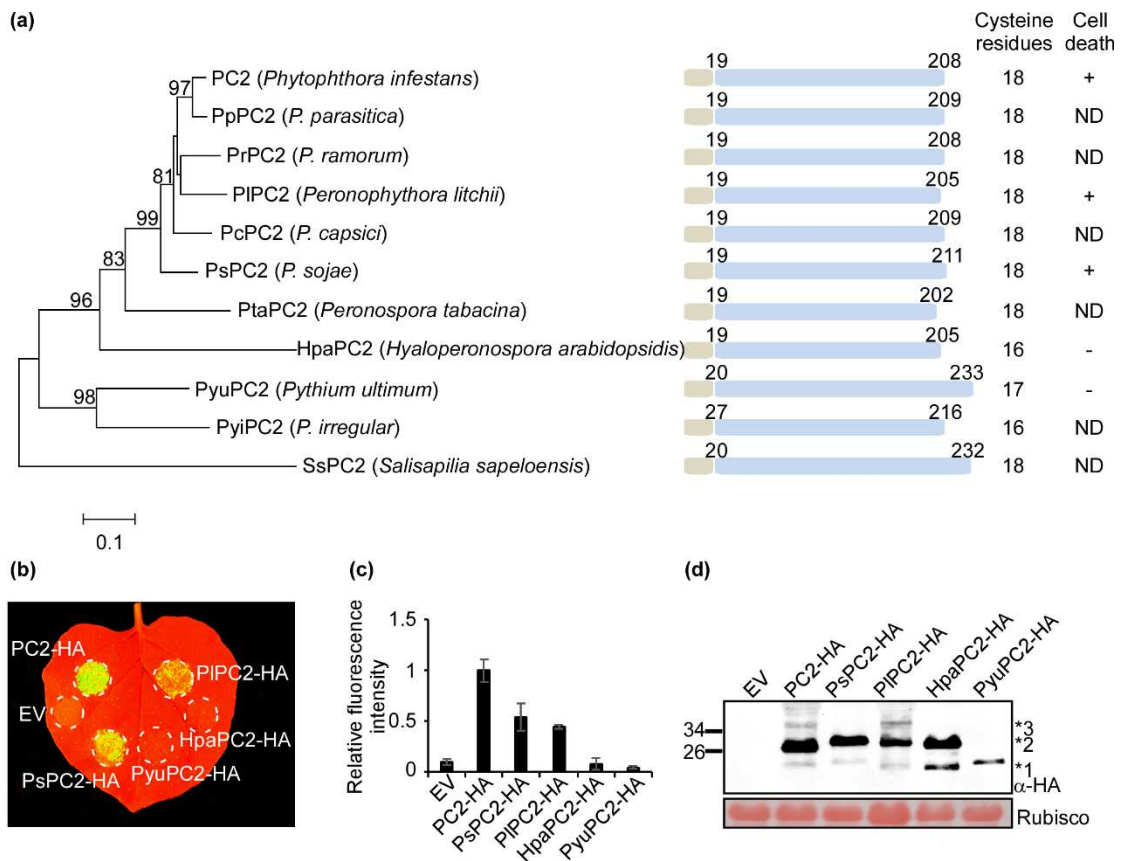


Fig. 3 PC2 homologs are widely present in oomycete species. (a) Phylogeny of PC2 from selected species. The tree was constructed by the neighbour-joining (NJ) algorithm implemented in MEGA7. Bootstrap percentage support for each branch is indicated. The scale bar represents 10% weighted sequence divergence. “+”, cell death induction in *N. benthamiana*; “-”, no cell death induction in *N. benthamiana*; “ND”, not determined. (b) to (c) PC2 homologs from *Phytophthora sojae* (PsPC2-HA) and *Peronophythora litchii* (PIPC2-HA) induced cell death in *N. benthamiana*. (b) Representative *N. benthamiana* leaves 5 days post-infiltration with *Agrobacterium* strains expressing PC2 homologs. (c) Quantification of the fluorescence intensity induced by PC2 homologs. The fluorescence intensity induced by PC2 was assigned the value 1.0. Means \pm SE from five independent replicates are shown. (d) Immunoblot analysis of PC2 or homologs fused with HA tags transiently expressed in *N. benthamiana* leaves.

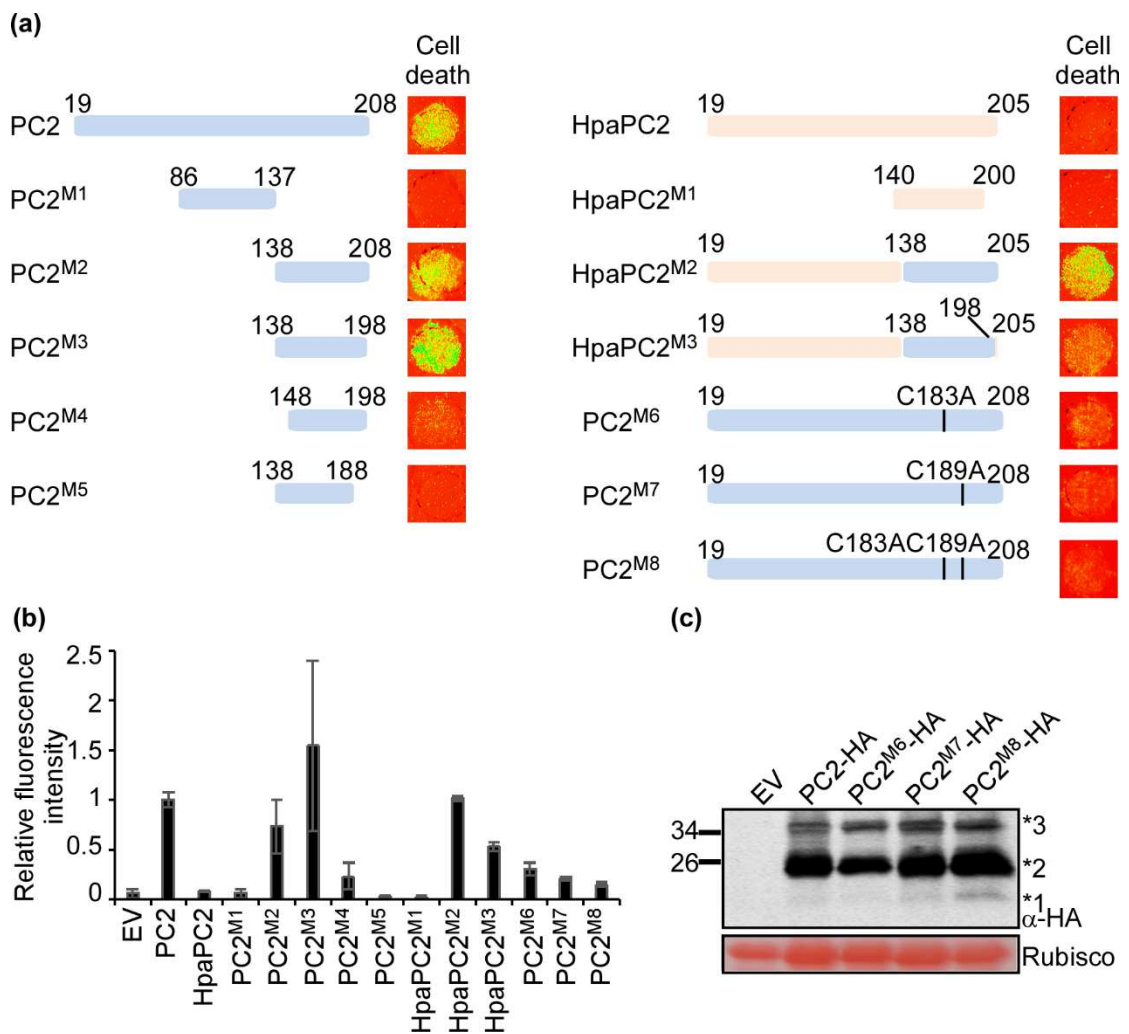


Fig. 4 PC2 protein sequence signatures that are required for cell death. (a) to (b) PC2^{M3}, a functional peptide that induce cell death. (a) Various PC2 mutants were constructed according to PC2 and HpaPC2 functional differentiation. Pictures were taken 5 days after infiltration with *Agrobacterium* strains carrying a series of mutants. (b) Quantification of the fluorescence intensity induced by different mutants in *N. benthamiana* leaves. The fluorescence intensity induced by PC2 was assigned the value 1.0. Means \pm SE from five independent replicates are shown. (c) Immunoblot analysis of PC2 mutants fused with HA tags transiently expressed in *N. benthamiana* leaves.

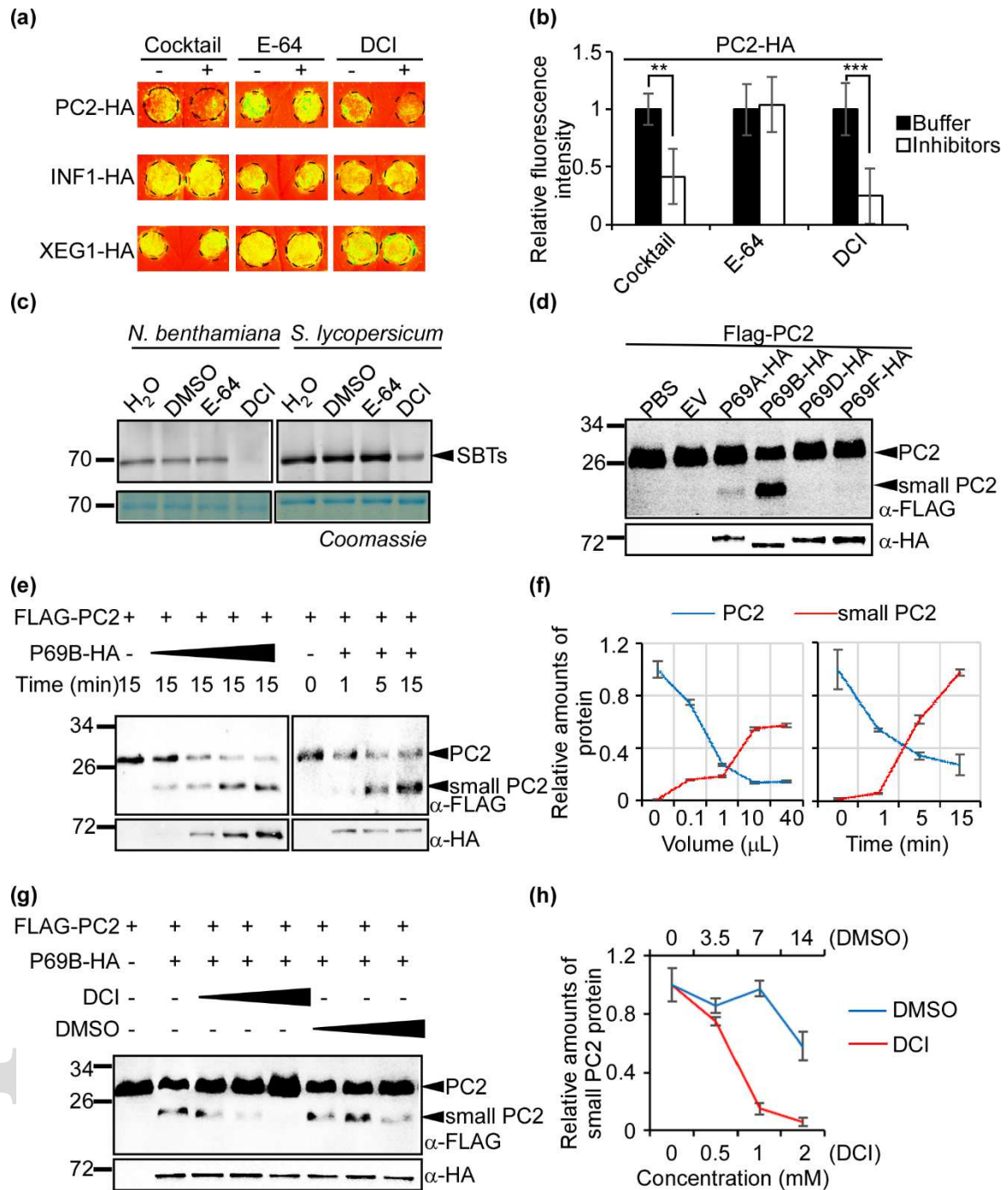


Fig. 5 Plant subtilase P69B cleaves PC2 protein. (a) to (b) PC2-induced cell death in *N. benthamiana* leaves was inhibited by plant protease inhibitor cocktail and serine protease inhibitor DCI. (a) Representative photographs. The *N. benthamiana* leaves were infiltrated with the cocktail and E-64 6 hours before agrobacterium-injected PC2, or DCI 12 hours after PC2 expression. E-64, a cysteine protease inhibitor, used as a control. (b) Quantification of PC2-induced fluorescence intensity in *N. benthamiana* leaves after treatment by chemical inhibitors. Fluorescence intensity triggered by PC2 under respective buffer treatment was assigned the value 1.0. Means \pm SE from six independent replicates are shown. Asterisks indicate significant differences (** $P < 0.01$; *** $P < 0.001$; one-way ANOVA). (c) DCI inhibits serine protease activity in tomato and *N. benthamiana* apoplastic fluids. The apoplastic fluids were incubated for 30 min with DCI. E-64 was used as a control. Active serine proteases were labelled using FP-Tamra. Labelled proteins were detected in a protein gel by fluorescent scanning. (d) The PC2 protein was cleaved by P69B in vitro. HA-tagged P69B or homologs were expressed in *N. benthamiana*, and FLAG-PC2-His protein was expressed in *E. coli*. PC2 and P69B or its homologs protein were co-incubated at 10°C for 30 minutes. The small band indicated PC2 cleavage products and were detected using anti-FLAG immunoblot. (e) to (f) Cleavage of PC2 was gradually increased after adding the various concentrations of P69B or the incubation time. (e) Representative photographs. (f) Quantification of the PC2 and small PC2 signals after incubation with P69B. Signals were quantified from Western blots with ImageJ. Means \pm SE from three independent replicates are shown. (g) to (h) Serine protease inhibitor DCI prevented P69B cleavage of PC2 protein. (g) Representative photographs. HA-tagged P69B protein was added into the tube after FLAG-tagged PC2 protein and DCI were co-incubate in 4°C for 30 minutes. The cleavage products were gradually reduced in the presence of 0.5 mM, 1 mM, and 2 mM DCI (according concentrations for DMSO are 3.5 mM, 7 mM, and 14 mM). The cleavage products were detected using anti-FLAG immunoblot. (h) Quantification of the small PC2 signals after different treatments. Signals were quantified from Western blots with ImageJ. Means \pm SE from three independent replicates are shown.

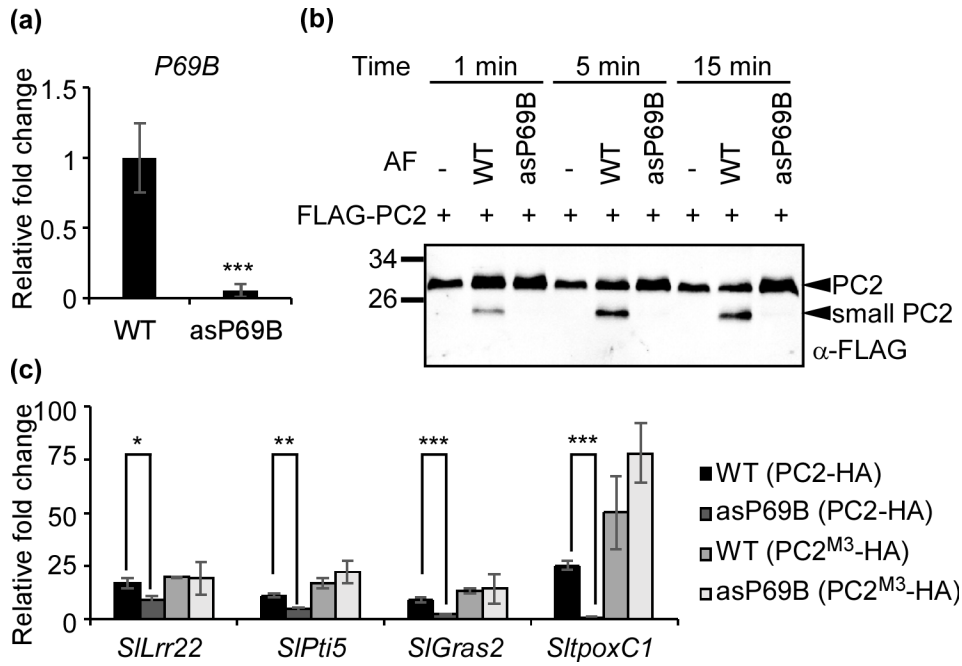


Fig. 6 Plant subtilase P69B is required for PC2-triggered immunity. (a) The *P69B* expression level in asP69B tomato determined by qRT-PCR. The *P69B* silenced transgenic tomato line (asP69B) was generated in the Money Maker (MM-Cf0, WT) background (Paulus *et al.*, 2020). Actin was used as an endogenous reference for normalization. Means \pm SE from three independent replicates are shown. Asterisks indicate significant differences (*** P < 0.001; one-way ANOVA). (b) Apoplastic fluid extracted from asP69B did not cleave PC2 protein. PC2 recombinant protein was co-incubated with the apoplastic fluids (AF) extracted from WT or asP69B tomato plants. Cleavage products were detected using anti-FLAG immunoblot. (c) PC2, not PC2^{M3}, induced up-regulation of tomato defense-related genes were impaired in asP69B plants. The gene expression was examined by qRT-PCR. Actin was used as an endogenous reference for normalization. The expression changes of *SILrr22*, *SIPti5* and *SIGras2* genes were detected 12 hours after PC2 expression and *SltpoxC1* is the result of 48 hours after PC2 expression. Means \pm SE from three independent replicates are shown. Asterisks indicate significant differences (* P < 0.05; ** P < 0.01; *** P < 0.001; one-way ANOVA).

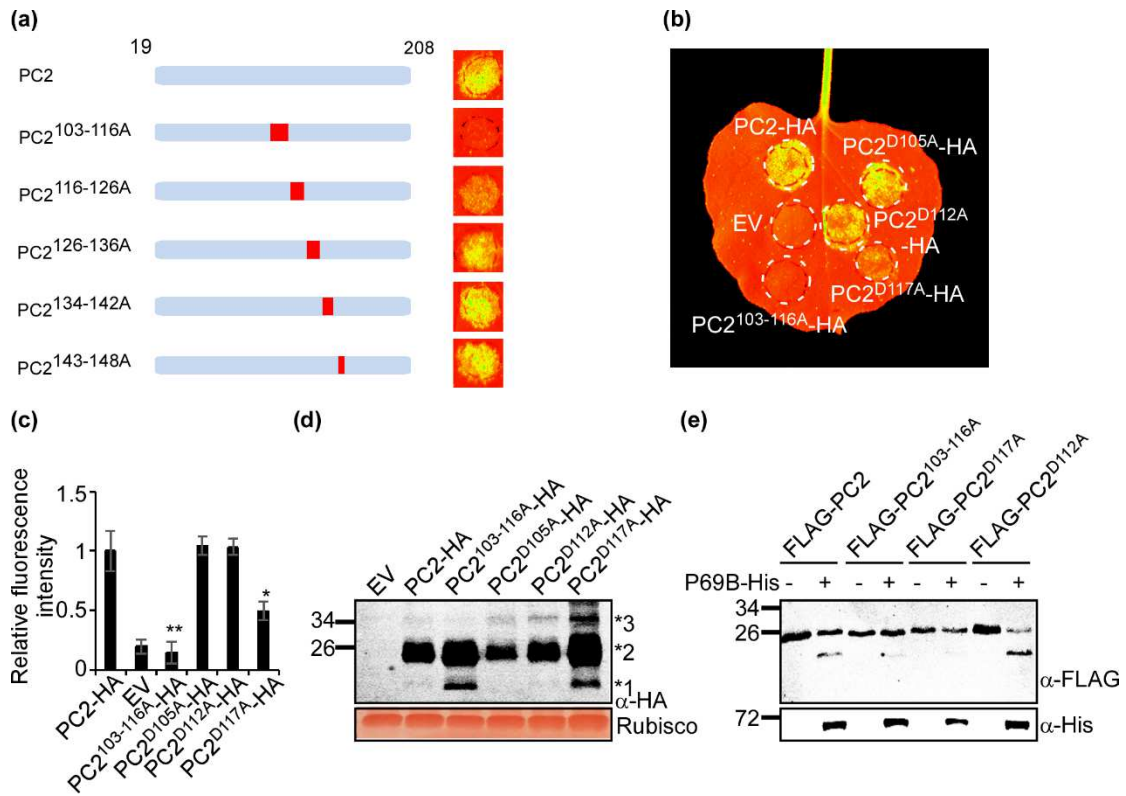


Fig. 7 Screen PC2 mutants that are resistant to P69B protease cleavage. (a) Mutant PC2^{103-116A} cannot induce cell death in *N. benthamiana*. A total of five mutants covering 46 amino acids from 103-148 are generated based on PC2 fragment. The numbers refer that all the residues in this region are substituted by alanine. All tested mutants were transiently expressed in *N. benthamiana* leaves by agroinfiltration. (b) to (c) PC2^{D117A} induce weakened cell death in *N. benthamiana*. (b) Representative photographs. Three mutants PC2^{D105A}, PC2^{D112A} and PC2^{D117A} that substituted the Asp to Ala residues in or around 103-116 region were created. All tested mutants were transiently expressed in *N. benthamiana* leaves by agroinfiltration. (c) Quantification of the fluorescence intensity induced by different mutants in *N. benthamiana* leaves. The fluorescence intensity induced by PC2 was assigned the value 1.0. Means \pm SE from three independent replicates are shown. Asterisks indicate significant differences (*P < 0.05; **P < 0.01; one-way ANOVA). (d) Immunoblot analysis of PC2 mutants fused with HA tag transiently expressed in *N. benthamiana* leaves. (e) PC2^{D117A} significantly reduced the cleavage under the P69B treatment. PC2 or the mutants' recombinant protein were co-incubated with purified P69B protein extracted from *N. benthamiana* leaves. Cleavage products were detected using anti-FLAG immunoblot.

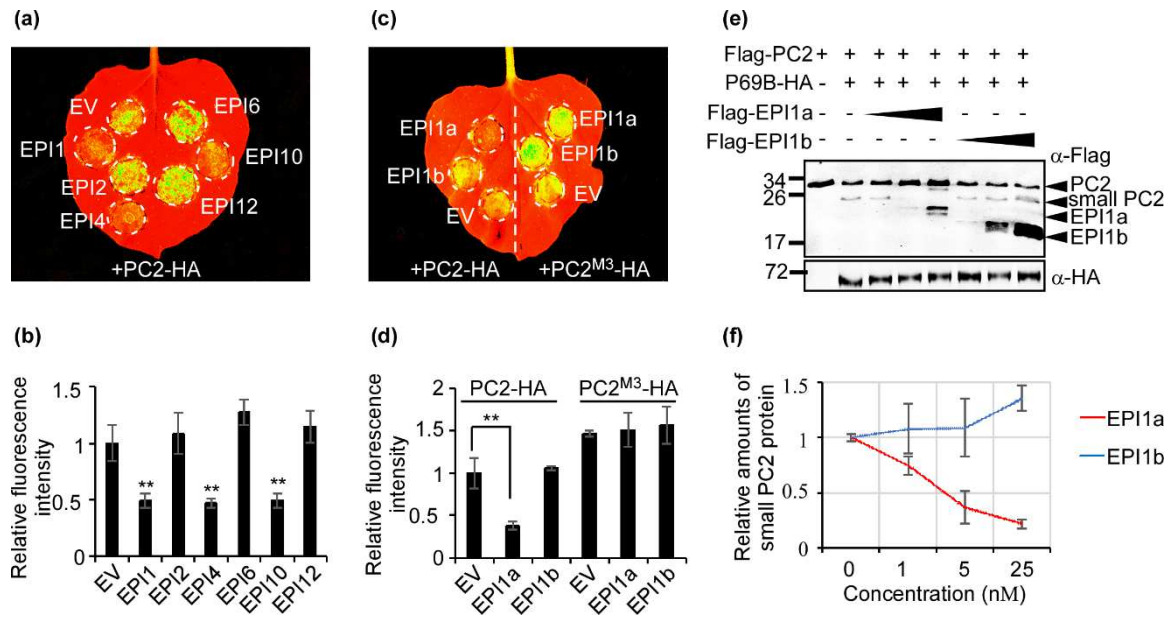


Fig. 8 Serine protease inhibitors secreted by *P. infestans* counteract PC2 cleavage. (a) to (b) PC2 induced cell death in *N. benthamiana* leaves was inhibited by *P. infestans* secreted serine protease inhibitor EPI1, EPI4 and EPI10. (a) Representative photographs. The *N. benthamiana* leaves were infiltrated with different EPIs 36 hours before PC2 expression. (b) Quantification of fluorescence intensity induced by PC2 in *N. benthamiana* leaves under different EPIs treatment. The PC2-elicited fluorescence with EV treatment was assigned the value 1.0. Means \pm SE from six independent replicates are shown. Asterisks indicate significant differences (** $P < 0.01$; one-way ANOVA). (c) to (d) Cell death induced by PC2, not PC2^{M3}, was inhibited by EPI1a. (c) Representative photographs. The *N. benthamiana* leaves were infiltrated with the EPI1a and EPI1b 36 hours before PC2 expression. (d) Quantification of fluorescence intensity induced by PC2 in *N. benthamiana* leaves after EPI1a treatment. The PC2-elicited fluorescence with EV treatment was assigned the value 1.0. Means \pm SE from six independent replicates are shown. Asterisk indicates significant differences (** $P < 0.01$; one-way ANOVA). (e) to (f) Recombinant EPI1a inhibits P69B cleavage of PC2 protein. (e) Representative photographs. FLAG-EPI1a and FLAG-EPI1b recombinant protein were expressed in *E. coli*. After the preincubation of P69B with EPI1a or EPI1b, PC2 protein was added into tubes. PC2 were gradually reduced in the presence of 0.5, 2.5, or 12.5 μ M purified EPI1a protein. EPI1b, a non-functional Kazal-like domain, served as a control. (f) Quantification of the small PC2 signals after different treatments. Signals were quantified from Western blots with ImageJ. Means \pm SE from three independent replicates are shown.